Insights into Hydrate Formation and Stability of Morphinanes from a Combination of Experimental and Computational Approaches

Doris E. Braun, Thomas Gelbrich, Volker Kahlenberg and Ulrich J. Griesser

Electronic Supporting Information

Contents of Supporting Information

A) Experimental

1. Nomenclature (Abbreviations)

Crystalline forms of the six investigated morphinanes were named as follows:

M	Morphine
C	Codeine
D	Ethylmorphine (Dionine)
Cl	Hydrochloride
I°, II, III	Anydrate form I°, II, III
°	Thermodynamic room temperature form
1H	Monohydrate
2H	Dihydrate
3H	Trihydrate
$_{calc}$	Calculated structure
Examples:	
M*Cl*-3H$_{calc}$	Calculated morphine hydrochloride trihydrate structure
C-I°	Codeine anhydrate form I°

2. Crystallization Experiments

8-10 mg of compound were used for each of the evaporation, cooling crystallization or vapor diffusion experiments. The used solvents were all of analytical quality and all organic solvents were purchased from Aldrich or Fluka. The crystallization products were analysed with (hot-stage) microscopy, differential scanning calorimetry, thermogravimetric analysis, IR spectroscopy and powder X-ray diffractometry.

Evaporation experiments (EV): A saturated solution (at RT) of the compound was filtered and the solvent was evaporated from a watch glass at RT.

Cooling crystallization experiments (CC): A hot saturated solution of the compound (close to the boiling point of each solvent) was either cooled fast to 4 °C or slowly (test tube wrapped in aluminum foil) to room temperature.

Vapor diffusion experiments (VD): A saturated solution of the compound at RT was placed in a small vial, which was placed upright in a larger closed vial in which a quantity of anti-solvent had been added.

2.1. Morphine (M)

Table S1. Results of morphine crystallization experiments (**M**-1H – monohydrate).

Solvent	Fast CC	Slow CC
Ethanol	**M**-1H	**M**-1H
Water	**M**-1H	**M**-1H

2.2. Morphine Hydrochloride (M*Cl*)

Table S2. Results of morphine hydrochloride crystallization experiments (**M***Cl*-3H – trihydrate).

Solvent	Fast CC	Slow CC
Ethanol	**M***Cl*-3H	**M***Cl*-3H
Water	**M***Cl*-3H	**M***Cl*-3H

2.3. Codeine (C)

Table S3. Results of codeine evaporation experiments (**C**-I° – anhydrate form I°, **C**-1H – monohydrate).

Solvent	Solid Form	Solvent	Solid Form
Methanol	**C**-I°	Chloroform	**C**-I°
Ethanol	**C**-I°	Dichloromethane	**C**-I°
1-Propanol	**C**-I°	Ethyl acetate	**C**-I°
2-Propanol	**C**-I°	1,4-Dioxane	**C**-I°
2-Butanol	**C**-I°	Dimethyl sulfoxide	**C**-I°
t-Penanol	**C**-I°	Dimethyl formamide	**C**-I°
Acetone	**C**-I°	Tetrahydrofurane	**C**-I°
Acetonitrile	**C**-I°	Toluene	**C**-I°
Nitromethane	**C**-I°	Water	**C**-1H

Table S4. Results of codeine crystallization experiments (**C**-I° – anhydrate form I°, **C**-1H – monohydrate).

Solvent	Fast CC	Slow CC
Methanol	**C**-I°	**C**-I°
Ethanol	**C**-I°	**C**-I°
Water	**C**-1H	**C**-1H
Methanol:Water (1:1)	**C**-1H	**C**-1H

Table S5. Results of codeine vapor diffusion experiments (**C**-I° – anhydrate form I°).

Solvent	Anit-solvent	Solid form
Dichloromethane	2-Pentane	**C**-I°

2.4. Codeine Hydrochloride (C*Cl*)

Table S6. Results of codeine HCl crystallization experiments (**C***Cl*-I° – anhydrate form I°, **C***Cl*-2H – dihydrate).

Solvent	Fast CC	Slow CC
Methanol	**C***Cl*-2H	**C***Cl*-2H
Ethanol	**C***Cl*-2H	**C***Cl*-2H
2-Propanol	**C***Cl*-I°	**C***Cl*-2H
1-Butanol	**C***Cl*-I°	**C***Cl*-I°
2-Butanol	**C***Cl*-I°	**C***Cl*-2H
1-Pentanol	**C***Cl*-I°	**C***Cl*-I°
t-Pentanol	**C***Cl*-I°	**C***Cl*-I°
Acetone:Water (1:1)	**C***Cl*-2H	**C***Cl*-2H
Acetonitrile	**C***Cl*-I°	**C***Cl*-I°
Ethyl acetate	**C***Cl*-2H	**C***Cl*-2H
Ethyl methyl ketone	**C***Cl*-I°	**C***Cl*-I°
1,4-Dioxane	**C***Cl*-2H	**C***Cl*-2H
Dimethyl formamide	**C***Cl*-I°	**C***Cl*-I°
Dimethyl sulfoxide	**C***Cl*-I°	**C***Cl*-I°

Table S7. Results of codeine HCl vapor diffusion experiments (**C***Cl*-2H – dihydrate).

Solvent	Anit-solvent	Solid form
Dichloromethane	2-Pentane	**C***Cl*-2H

2.5. Ethylmorphine (D)

Table S8. Results of ethylmorphine crystallization experiments (**D**-1H – monohydrate).

Solvent	Fast CC	Slow CC
Methanol	**D**-1H	**D**-1H
Ethanol	**D**-1H	**D**-1H
2-Propanol	**D**-1H	**D**-1H
1-Butanol	**D**-1H	**D**-1H
t-Pentanol	**D**-1H	**D**-1H
Acetone	**D**-1H	**D**-1H
Acetonitrile	**D**-1H	**D**-1H
Dichloromethane	**D**-1H	**D**-1H
Chloroform	**D**-1H	**D**-1H
Cyclohexanone	**D**-1H	**D**-1H
Methyl acetate	**D**-1H	**D**-1H
Ethyl acetate	**D**-1H	**D**-1H
Ethyl methyl ketone	**D**-1H	**D**-1H
1,4-Dioxane	**D**-1H	**D**-1H
Dimethyl formamide	**D**-1H	**D**-1H
Dimethyl sulfoxide	**D**-1H	**D**-1H
Nitromethane	**D**-1H	**D**-1H
Pyridine	**D**-1H	**D**-1H
Glycerol	**D**-1H	**D**-1H
Water	**D**-1H	**D**-1H

Table S9. Results of ethylmorphine vapor diffusion experiments (**D**-1H – monohydrate).

Solvent	Anit-solvent	Solid form
Dichloromethane	2-Pentane	**D**-1H
Dichloroethane	2-Pentane	**D**-1H

2.6. Ethylmorphine Hydrochloride (D*Cl*)

Table S10. Results of ethylmorphine HCl evaporation experiments (**D***Cl*-2H – dihydrate).

Solvent	Solid Form	Solvent	Solid Form
Methanol	amorphous	Dioxane	amorphous
Ethanol	amorphous > **D***Cl*-2H	Dimethyl formamide	amorphous
2-Propanol	amorphous + **D***Cl*-2H	Dimethyl sulfoxide	amorphous
Water	**D***Cl*-2H > amorphous	Nitromethane	amorphous > **D***Cl*-2H
Acetone	amorphous > **D***Cl*-2H	Tetrahydrofurane	amorphous
Acetonitrile	amorphous > **D***Cl*-2H	Acetic Acid	amorphous
Chloroform	amorphous + **D***Cl*-2H		

Table S11. Results of ethylmorphine HCl crystallization experiments (**D***Cl*-2H – dihydrate).

Solvent	Fast CC	Slow CC
Methanol	**D***Cl*-2H	**D***Cl*-2H
Ethanol	**D***Cl*-2H	**D***Cl*-2H
2-Propanol	**D***Cl*-2H	**D***Cl*-2H
1-Butanol	**D***Cl*-2H	**D***Cl*-2H
2-Butanol	**D***Cl*-2H	**D***Cl*-2H
t-Pentanol	**D***Cl*-2H	**D***Cl*-2H
Acetone	**D***Cl*-2H	**D***Cl*-2H
Acetonitrile	**D***Cl*-2H	**D***Cl*-2H
Chloroform	amorphous	amorphous
Ethyl acetate	**D***Cl*-2H	**D***Cl*-2H
Ethyl methyl ketone	**D***Cl*-2H	**D***Cl*-2H
Toluene	**D***Cl*-2H	**D***Cl*-2H
Water	**D***Cl*-2H	**D***Cl*-2H

Table 12. Results of ethylmorphine HCl vapor diffusion experiments (**D***Cl*-2H – dihydrate).

Solvent	Anit-solvent	Solid form
Dichloromethane	2-Pentane	**D***Cl*-2H
Dichloroethane	2-Pentane	**D***Cl*-2H

3. Gravimetric Moisture Sorption/Desorption Analysis (GMS)

Details of the experimental setup of the gravimetric moisture sorption/desorption studies are given in Table S13. Additional sorption/desorption isotherms are given for **M***Cl* (Figure S1) and **C** (Figure S2).

Table S13. Experimental setup of gravimetric moisture sorption/desorption studies.

Setup 1 (M, C, D, M*Cl*, C*Cl*, D*Cl*)				
Cycle Number	**RH% (start)**	**RH% (end)**	**Number of steps**	**Time (h)**
1	40	30	1	
2	25	10	2	
3	9	5	4	
4	6	10	4	
5	12	30	9	
6	35	95	12	
7	90	50	4	
8	45	10	7	
9	5	0	1	120
10	5	40	7	
11	50	90	4	
12	95	90	1	
13	80	40	4	
Setup 2 (M, C, M*Cl*, C*Cl*)				
Cycle Number	**RH% (start)**	**RH% (end)**	**Number of steps**	**Time (h)**
1	0	0	1	12
2	0	90	18	
3	95	90	1	
4	85	0	17	
5	5	40	7	
Setup 3 (M, C*Cl*)				
Cycle Number	**RH% (start)**	**RH% (end)**	**Number of steps**	**Time (h)**
1	40	0	4	
2	10	90	8	
3	80	0	8	
4	10	40	3	

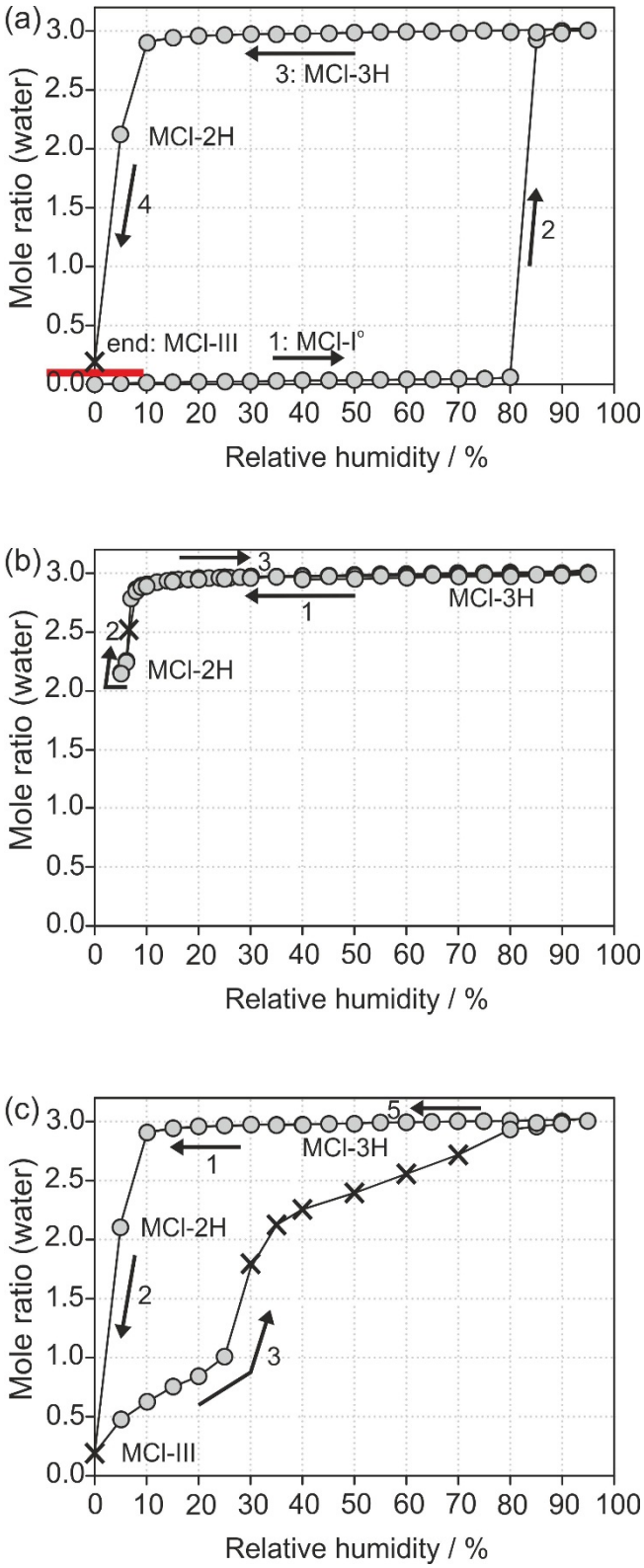

Figure S1. Moisture sorption and desorption curves of **M***Cl* at 25 °C: The grey circles present data points that fullfill the preset equilibrium conditions (see experimental section), whereas the crosses mark measurement values that did not reach the equilibrium within the allowed time limit (48 h). The numbers indicate the order of subsequent sorption (increasing RH) and desorption (decreasing RH) cycles.

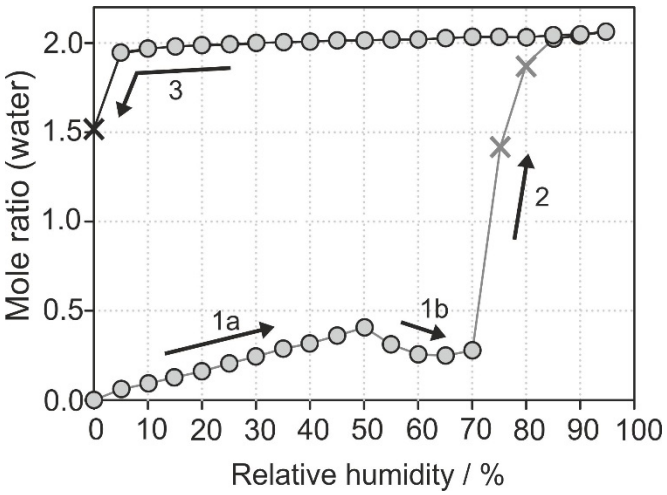

Figure S2. Moisture sorption and desorption curves of **C** starting from **C**-I° contaminated with amorphous codeine at 25 °C: The grey circles present data points that fullfill the preset equilibrium conditions (see experimental section), whereas the crosses mark measurement values that did not reach the equilibrium within the allowed time limit (48 h). The numbers indicate the order of subsequent sorption (increasing RH) and desorption (decreasing RH) cycles.

4. Determination and Analysis of Crystal Structures

4.1. Crystallographic Data

Table S14. Crystallographic data and details of crystal structure determinations.

Phase designator	**C**-1H	**D**-1H	**C***Cl*-I°	**C***Cl*-2H	**D***Cl*-2H
Empirical formula	$C_{18}H_{21}NO_3 \cdot H_2O$	$C_{19}H_{23}NO_3 \cdot H_2O$	$C_{18}H_{22}NO_3^+ \cdot Cl^-$	$C_{18}H_{22}NO_3^+ \cdot Cl^- \cdot 2(H_2O)$	$C_{19}H_{24}NO_3^+ \cdot Cl^- 2(H_2O)$
Formula weight	317.37	331.40	335.82	371.85	385.87
Temperature / K	173(2)	173(2)	173(2)	123(2)	123(2)
Wavelength / Å	Cu *K*α	Mo *K*α	Mo *K*α	Mo *K*α	Cu *K*α
Crystal size /mm	0.36 × 0.32 × 0.27	0.40 × 0.28 × 0.26	0.32 × 0.3 × 0.25	0.17 × 0.05 × 0.03	0.14 × 0.04 × 0.02
Crystal system	orthorhombic	orthorhombic	orthorhombic	orthorhombic	orthorhombic
Space group	$P2_12_12_1$	$P2_12_12_1$	$P2_12_12_1$	$P2_12_12_1$	$P2_12_12_1$
a/ Å	10.3994(2)	7.08246(18)	7.14435(17)	6.7621(5)	6.8715(2)
b/ Å	12.5671(2)	13.1493(3)	13.2304(3)	12.9315(9)	13.3924(4)
c/ Å	12.0640(2)	18.0581(5)	16.5408(4)	20.3080(14)	20.4176(5)
Volume/ Å^3	1576.65(5)	1681.74(7)	1563.48(6)	1775.8(2)	1878.95(9)
Z	4	4	4	4	4
Density (calc)/ g cm^{-3}	1.337	1.309	1.427	1.391	1.364
Absorption coefficient	0.77	0.09	0.26	0.24	2.06
Absolute structure parameter	0.02(8)	–	–0.11(5)	-0.01(5)	0.017(10)
Theta range for data collection / °	5.1 to 67.5	3.1 to 26.0	3.1 to 26.0	2.55 to 26.0	5.4 to 67.7
Index ranges	–12<=h<=12, –14<=k<=15, –14<=l<=14	–8<=h<=8, –16<=k<=16, –22<=l<=20	–8<=h<=6 –15<=k<=16, –19<=l<=20	–8<=h<=8, –13<=k<=15, –25<=l<=25	–8<=h<=8, –16<=k<=14, –23<=l<=24
No. of measured, independent and observed [$I > 2\sigma(I)$] reflections	9716/2833/2771	11519/3295/3121	12628/3062/2897	17583/3492/3291	10707/3360/3153
Refinement method	Full-matrix least-squares on F^2				
Data/ parameters/ restraints	2833 / 223 / 2	3295 / 232 / 0	3062 / 218/ 2	3492 / 272 / 0	3360 / 259 / 8
Goodness-of-fit	1.04	1.05	1.05	1.03	0.98
Final R indices [I>2sigma(I)]	*R*1 = 0.0300, *wR*2 = 0.0782	*R*1 = 0.0308, *wR*2 = 0.0725	*R*1 = 0.0298, *wR*2 = 0.0727	*R*1 = 0.0257, *wR*2 = 0.0637	*R*1 = 0.0397, *wR*2 = 0.1055
R indices (all data)	*R*1 = 0.0307, *wR*2 = 0.0789	*R*1 = 0.0334, *wR*2 = 0.0738	*R*1 = 0.0320, *wR*2 = 0.0739	*R*1 = 0.0287, *wR*2 = 0.0647	*R*1 = 0.0431, *wR*2 = 0.1085
Largest diff. peak and hole	0.22, −0.14	0.16, −0.15	0.24, −0.17	0.22, −0.17	0. 58, −0.25

4.2. Treatment of H Atoms

Table S15. Treatment of H atoms (P = refinement of atomic positions; T = refinement of isotropic thermal displacement parameters, Uiso; m = morphinane; re = distance restraints; F = free refinement)

H-position(s)		**C**-1H	**D**-1H	**C***Cl*-I°	**C***Cl*-2H	**D***Cl*-2H
–CH, –CH_2	**P**	riding model	riding model	riding model	riding model	riding model
	T	U_{iso} = 1.2U_{eq}(C)	U_{iso} = 1.2U_{eq}(C)	U_{iso} = 1.2U_{eq}(C)	free	U_{iso} = 1.2U_{eq}(C)
–CH_3	**P**	riding model	riding model	riding model	riding model	riding model
	T	U_{iso} = 1.5U_{eq}(C)	U_{iso} = 1.5U_{eq}(C)	U_{iso} = 1.5U_{eq}(C)	free	U_{iso} = 1.5U_{eq}(C)
–OH (*m*)	**P**	R: O–H = 0.82(2) Å	free	re: N–H = 0.82(2) Å	free	riding model
	T	F	free	free	free	U_{iso} = 1.5U_{eq}(O)
H_2O	**P**	R: O–H = 0.82(2) Å	free	–	free	re: O–H = 0.86(2) Å[a]
	T	F	free	–	free	free / U_{iso} = 1.2 U_{eq}(O)
–NH	**P**	–	–	re: N–H = 0.86(2) Å	free	free
	T	–	–	free	free	free

[a]Location of water proton positions derived from electronic structure calculations (DFT-TS, see section 11).

4.3. *XPac* Comparison of Experimental Crystal Structures

4.3.1. General

Crystal packing comparisons were carried out using the program *XPac*[1] and quantitative dissimilarity parameters were generated in the previously described manner.[2] The pairwise comparisons of crystal structures were based on geometrical parameters generated from the positions of 20 atoms of the morphinane moiety (all non-H atoms except for C17 and those of R, see Figure 1). Water molecules and chloride anions have not been considered in this analysis.

An overview of packing relationships is given in Figrue S3 and parameters associate with common supramolecular constructs[1] (SCs) identified in this study are collected in Tables S16-S20.

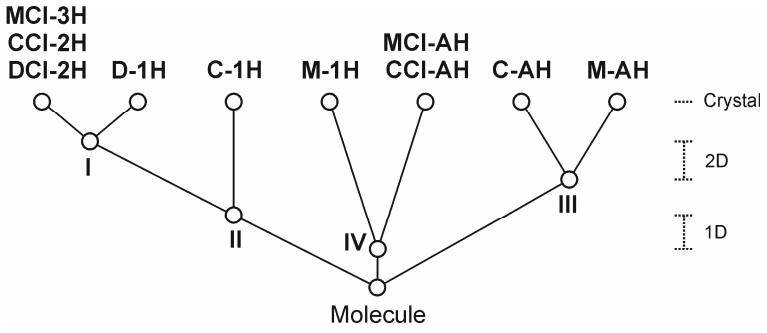

Figure S3. Overview of packing relationships between substructures composed of morphinane moieties of solid forms of morphine (**M**), codeine (**C**) and dionine (**D**), based on an *XPac* study.

4.3.2. **Subset: D***Cl*-2H, **C***Cl*-2H **M***Cl*-3H, **D**-1H and **C**-1H

Table S16. Parameters associated 2D SCs **I** and **II** and with the isostructurality of the hydrochloride hydrates **D***Cl*-2H, **C***Cl*-2H and **M***Cl*-3H: lattice directions t1, t2 and t3 and corresponding *d* values (Å); ∠(t1, t2) = ∠(t1, t2) = ∠(t2, t3) = 90°.

Structure	t1	t2	t3	SCs
D*Cl*-2H	100 / 6.872	010 / 13.392	001 / 20.418	**I**, **II**
C*Cl*-2H	100 / 6.762	010 / 12.932	001 / 20.308	**I**, **II**
M*Cl*-3H	$00\bar{1}$ / 6.941	$\bar{1}00$ / 13.019	010 / 20.750	**I**, **II**
D-1H	$\bar{1}00$ / 7.082	$0\bar{1}0$ / 13.149	–	**I**, **II**
C-1H	–	001 / 12.064	–	**II**

Table S17. *XPac* dissimilarity parameters for the 2D SC **I** and **II** and for the series of isostructures **D***Cl*-2H, **C***Cl*-2H and **M***Cl*-3H (*n* = number of surrounding molecules in a cluster which defining an SC).

Structure 1	Structure 2	x_1 (SC **II**; *n* = 4)	x_2 (SC **I** *n* = 8)	x_3 (complete)
D*Cl*-2H	**C***Cl*-2H	6.0	5.2	5.4
D*Cl*-2H	**M***Cl*-3H	10.6	9.6	9.9
D*Cl*-2H	**D**-1H	3.7	4.1	–
D*Cl*-2H	**C**-1H	9.8	–	–
C*Cl*-2H	**M***Cl*-3H	4.8	4.3	4.8
C*Cl*-2H	**D**-1H	5.9	5.7	–
C*Cl*-2H	**C**-1H	7.9	–	–
M*Cl*-3H	**D**-1H	9.8	9.1	–
M*Cl*-3H	**C**-1H	9.3	–	–
D-1H	**C**-1H	7.0	–	–

4.3.3. **Subset: M***Cl*-I°, **C***Cl*-I° and **M**-1H

Table S18. Parameters associated 1D SC **VI** and with the isostructurality of **M**-1H and **M***Cl*-I°: lattice directions t4, t5 and t6 and corresponding *d* values (Å); ∠(t4, t5) = ∠(t4, t6) = ∠(t5, t5) = 90°.

Structure	t4	t5	t6	SC
M*Cl*-I°	$00\bar{1}$ / 7.350	$\bar{1}00$ / 12.852	010 / 16.037	**IV**
C*Cl*-I°	100 / 7.144	010 / 13.230	001 / 16.541	**IV**
M-1H	100 / 7.431	–	–	**IV**

Table S19. *XPac* dissimilarity parameters for the 1D SC **IV** and for isostructures **D***Cl*-2H, **C***Cl*-2H and **M***Cl*-3H (*n* = number of surrounding molecules in a cluster which defining an SC).

Structure 1	Structure 2	x_1 (*n* = 2)	x_2 (complete)
M*Cl*-I°	**M**-1H	8.1[a]	–
C*Cl*-I°	**M**-1H	10.7	–
M*Cl*-I°	**C***Cl*-I°	5.9	8.0[a]

[a] For a detailed discussion of this relationship, see ref. 3.

4.3.4. Subset: **C** and **M**-I°

Table S20. Corresponding lattice direction t7 and t8 and corresponding *d* values (Å) associated with the 2D SC **III** (t7 and t8 form an angle of 90°). Parameters associated 2D SC **III**: lattice directions t7 and t8 and the corresponding *d* values (Å); ∠(t7, t8) = 90°. The dissimilarity index *x* for the two instances of SC **III** in **C** and **M**-I° and is 4.7 (for *n* = 8).

Structure	t7	t8	SC
C	100 / 7.491	001 / 14.775	**III**
M-I°	100 / 7.699	001 / 13.740	**III**

4.4. Geometry of Classical Hydrogen Bonds

Table S21. Hydrogen bonding data of the free base structures.

Cpd.[a]	C_3–O_1H			C_6–O_3H			H_2O (Water)			NW[d]
	H-bond	GS[c]	*d* (O···X)/ Å	H-bond	GS[c]	*d* (O···X)/ Å	H-bond	GS[c]	*d* (O···O)/ Å	
M-AH	O_2–H···O_3	$C_1^1(8)$	2.757	O_3–H···O_1	$S_1^1(5)$	2.629	–	–	–	1D
M-MH	O_2–H···N	$C_1^1(9)$	2.635	O_3–H···O_W	$D_1^1(2)$	2.702	O_W–H···O_2	$D_1^1(2)$	2.966	3D
							O_W–H···O_3	$D_1^1(2)$	2.795	
C-AH	–	–	–	O_3–H···O_1	$S_1^1(5)$	2.643	–	–	–	
C-MH	–	–	–	O_3–H···N	$C_1^1(8)$	2.817	O_W–H···O_2	$D_1^1(2)$	3.118	1D
							O_W–H···O_3	$D_1^1(2)$	2.925	
*c*D-AH[b]	–	–	–	O_3–H···N	$C_1^1(8)$	2.748	–	–	–	1D
D-MH	–	–	–	O_3–H···N	$C_1^1(8)$	2.775	O_W–H···O_2	$D_1^1(2)$	2.985	1D
							O_W–H···O_3	$D_1^1(2)$	2.886	

[a]Compound, [b]computationally generated structure, [c]graph-set motif, [d]dimensionality of hydrogen-bonding network.

Table S22. Hydrogen bonding data of the HCl salts.

Cpd.[a]	C_3–O_1H			C_6–O_3H			N^+H			H_2O (Water)			NW[e]
	H-bond	GS[c]	*d*(O···X)/Å	H-bond	GS[c]	*d*(O···X)/Å	H-bond	GS[c]	*d*(N···X)/Å	H-bond[d]	GS[c]	*d*(O···X)/ Å	
MCl-AH	O_2–H···Cl	$D_1^1(2)$	3.158	O_3–H···Cl	$D_1^1(2)$	3.142	N–H···Cl	$D_1^1(2)$	3.062	–	–	–	1D
MCl-TH	O_2–H···O_{WC}	$D_1^1(2)$	2.821	O_3–H···O_1	$S_1^1(5)$	2.717	N–H···O_3	$C_1^1(8)$	2.799	O_{WA}–H···O_2	$D_1^1(2)$	2.557	3D
	–	–	–	–	–	–	–	–	–	O_{WA}–H···Cl	$D_1^1(2)$	3.156	
	–	–	–	–	–	–	–	–	–	O_{WB}–H···O_{WA}	$D_1^1(2)$	2.697	
	–	–	–	–	–	–	–	–	–	O_{WB}–H···Cl	$D_1^1(2)$	3.118	
	–	–	–	–	–	–	–	–	–	O_{WC}–H···O_3	$D_1^1(2)$	2.813	
	–	–	–	–	–	–	–	–	–	O_{WC}–H···Cl	$D_1^1(2)$	3.239	
CCl-AH	–	–	–	O_3–H···Cl	$D_1^1(2)$	3.141	N–H···Cl	$D_1^1(2)$	3.032	–	–	–	1D
CCl-DH	–	–	–	O_3–H···O_{w1}	$D_1^1(2)$	2.750	N–H···O_3	$C_1^1(8)$	2.747	O_{WB}–H···Cl	$D_1^1(2)$	3.223	3D
	–	–	–	–	–	–	–	–	–	O_{WB}–H···Cl	$D_1^1(2)$	3.247	
	–	–	–	–	–	–	–	–	–	O_{WC}–H···O_2	$D_1^1(2)$	2.890	
	–	–	–	–	–	–	–	–	–	O_{WC}–H···Cl	$D_1^1(2)$	3.125	
*c*DCl-AH[b]	–	–	–	O_3–H···Cl	$D_1^1(2)$	3.115	N–H···Cl	$D_1^1(2)$	3.033	–	–	–	1D
DCl-DH	–	–	–	O_3–H···O_{w1}	$D_1^1(2)$	2.804	N–H···O_3	$C_1^1(8)$	2.754	O_{WB}–H···Cl	$D_1^1(2)$	3.303	3D
	–	–	–	–	–	–	–	–	–	O_{WB}–H···Cl	$D_1^1(2)$	3.399	
	–	–	–	–	–	–	–	–	–	O_{WC}–H···O_2	$D_1^1(2)$	2.942	
	–	–	–	–	–	–	–	–	–	O_{WC}–H···Cl	$D_1^1(2)$	3.217	

[a]Compound, [b]computationally generated structure, [c]graph-set motif, [d]Water positions according to Figure 10, [e]dimensionality of hydrogen-bonding network.

4.5. Packing Diagrams

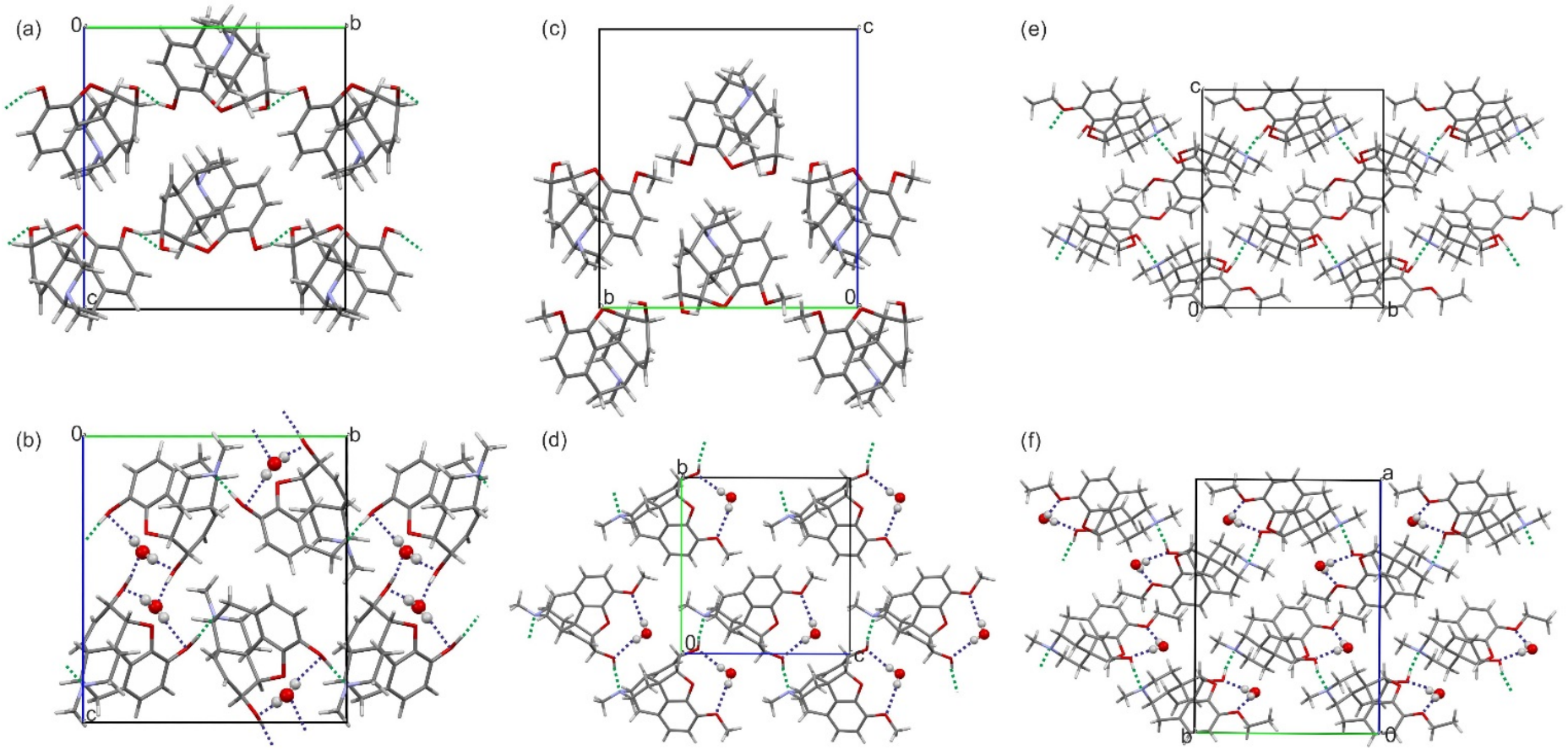

Figure S4. Packing diagrams of (a) **M**-I°,[4] (b) **M**-1H,[5] (c) **C**-I°,[6] (d) **C**-1H, (e) **D**-AH, and (f) **D**-I_{calc}. Hydrogen bonds are depicted with dotted lines.

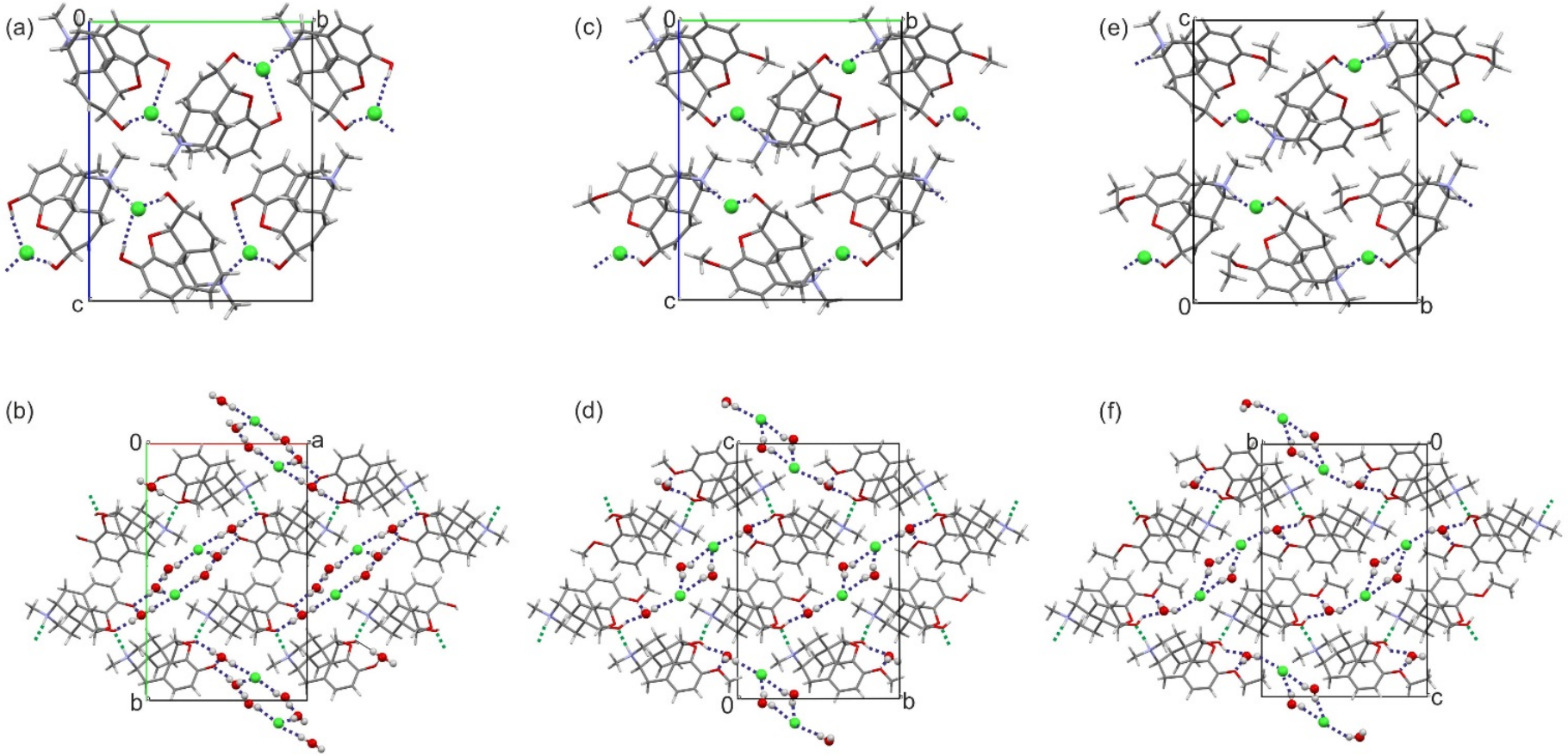

Figure S5. Packing diagrams of (a) **M***Cl*-I°,[3] (b) **M***Cl*-3H,[7] (c) **C***Cl*-I°, (d) **C***Cl*-2H, (e) **D***Cl*-I°$_{calc}$, and (f) **D***Cl*-2H. Hydrogen bonds are depicted with dotted lines.

5. Powder X-ray Diffraction

PXRD patterns of different solid forms of the six investigated morphinanes are given in Figure S6.

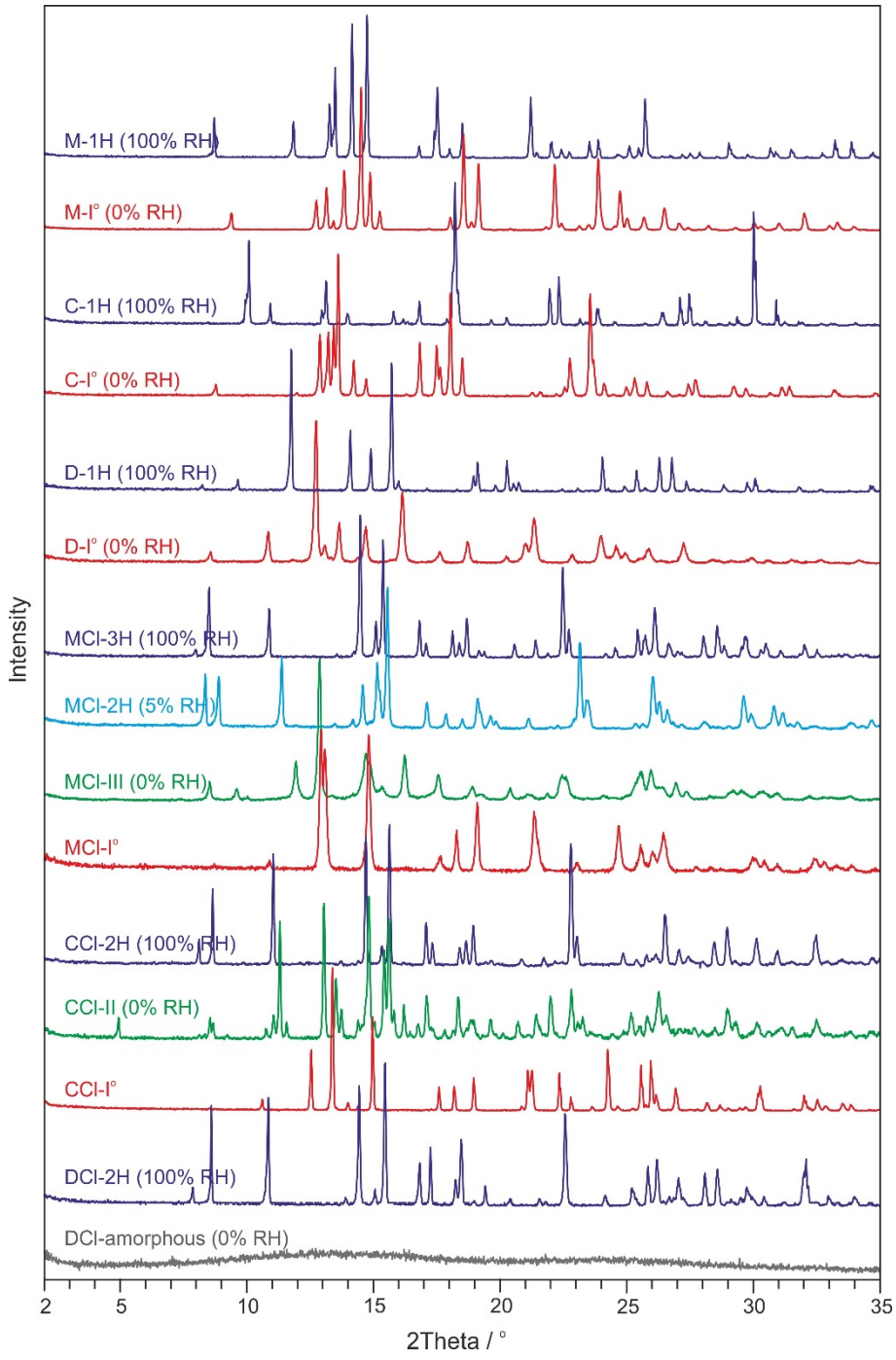

Figure S6. PXRD patterns of morphinane solid forms. Hydrate phases in blue and violet, stable anhydrate in red, unstable anhydrates in green and amorphous in grey.

Selected PXRD patterns used for constructing the Guinier plots (Figure 5) are given below (Figure S7).

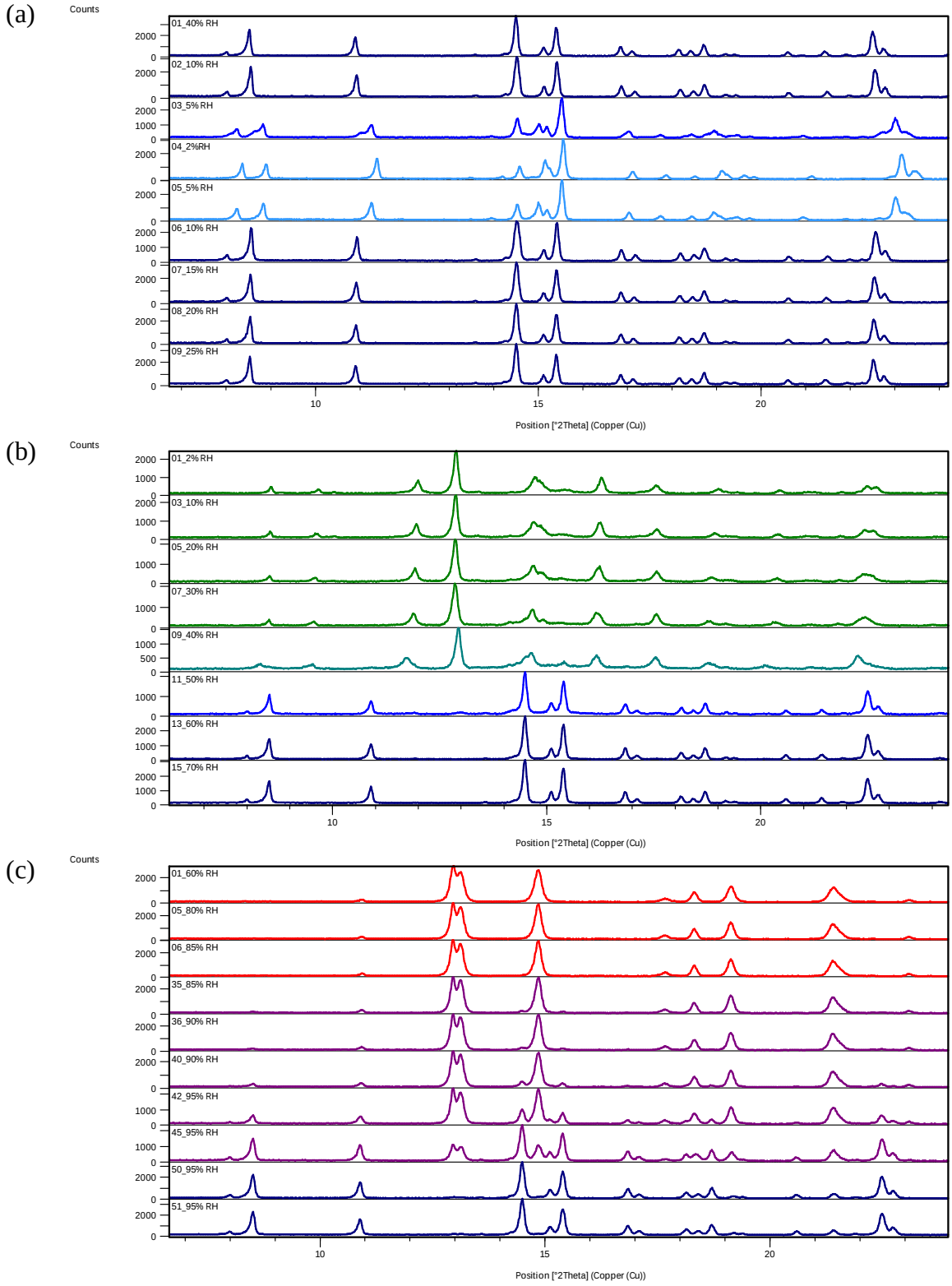

Figure S7. Moisture dependent PXRD measurements of **M***Cl*: starting with (a) **M***Cl*-3H, (b) **M***Cl*-III, and (c) **M***Cl*-I°. Numbers indicate the order and RH settings of the measurements.

6. Hot-stage Microscopy

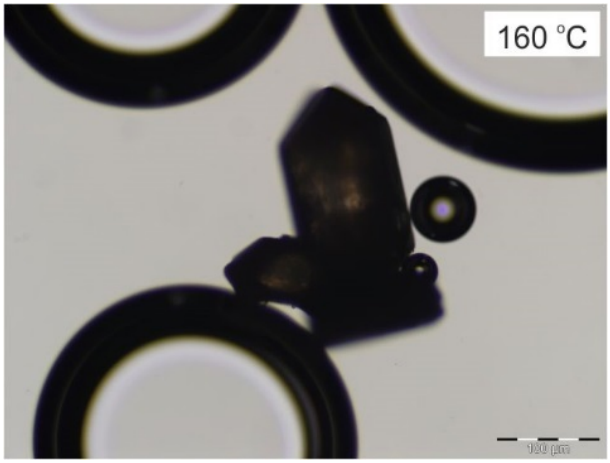

Figure S8. M-1H crystals embedded in silicon oil showing the formation of bubbles, i.e. **M**-1H to **M**-I° phase transformation.

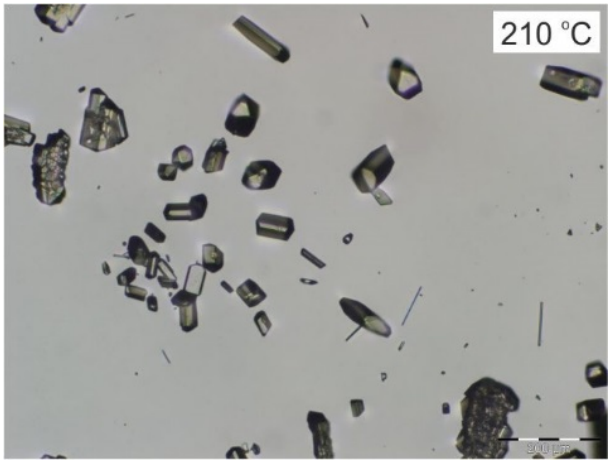

Figure S9. Morphine sublimates. Note that all of the crystals correspond to the same polymorphic form, **M**-I°.

7. Morphine (M): Differential Scanning Calorimetry + Powder X-ray Diffraction

M-1H was heated in 1-pinholed DSC pans at a heating rate of 20 °C min^{-1} (Figure S10). Measurements were stopped at predefined temperatures and the samples analysed with PXRD (Figure S11). The measurements confirmed the hydrate peritectic melting at 201.3±0.5 °C (dehydration was not complete at 180 °C, a mixture of **M**-1H and **M**-I° was present), and that the peak splitting at 260 °C can be attributed to melting and decomposition rather than the presence of two polymorphs (only one phase present at 230 °C).

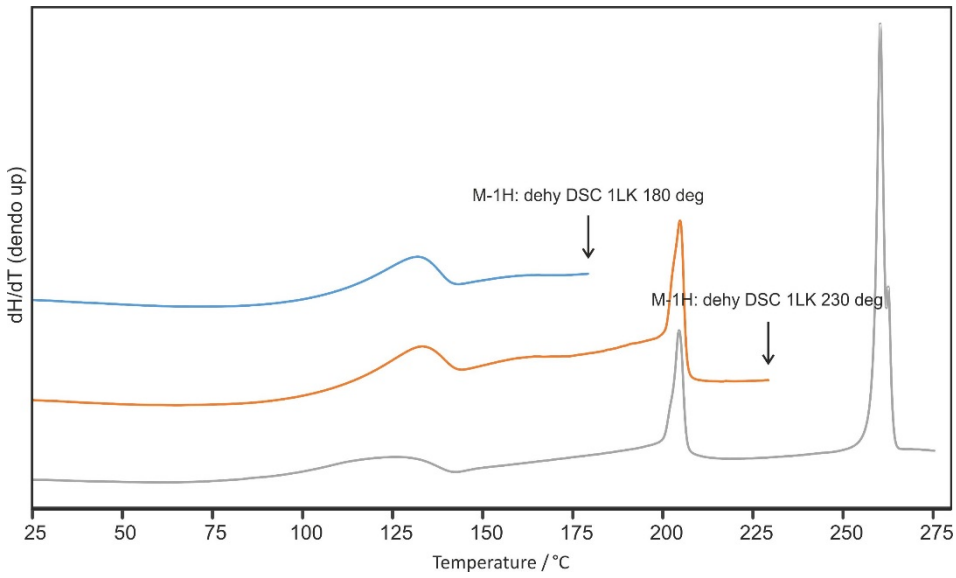

Figure S10. DSC thermograms of **M**-1H using a heating rate of 20 °C min^{-1}.

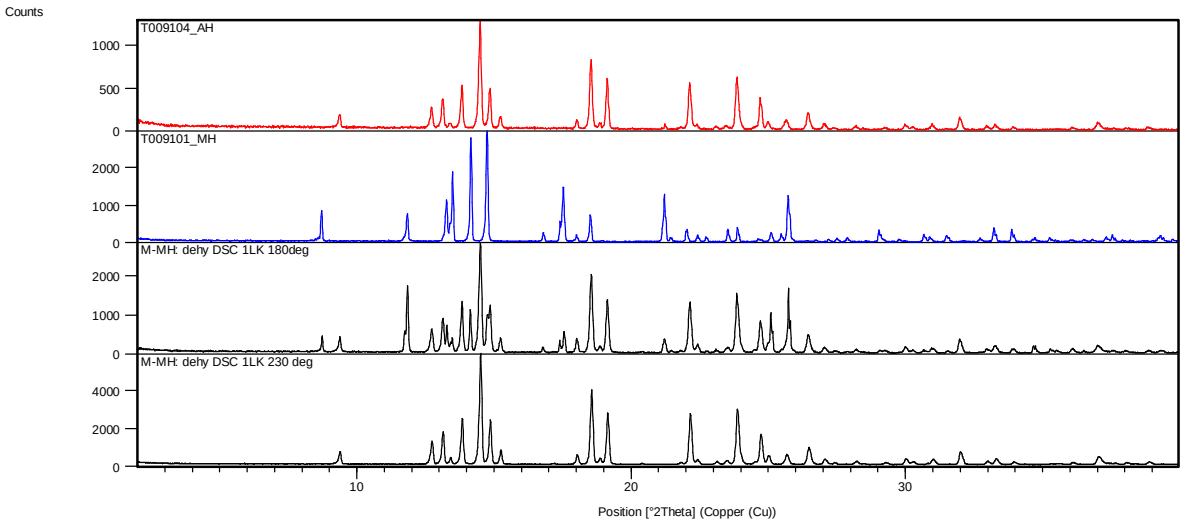

Figure S11. PXRD patterns of: **M**-I° (1st), **M**-1H (2nd), **M**-1H heated to 180 °C (3rd) and to 230 °C (4th).

8. Ethylmorphine (D): Infrared Spectroscopy

Infrared spectra of **D** (Figure S12) were recorded with a ZnSe ATR crystal (MIRacle, PIKE Technologies, Inc., USA) on a Perkin Elmer Spectrum GX (Perkin Elmer, Norwalk Ct., USA) over a range of 4000 to 600 cm^{-1} with a resolution of 2 cm^{-1} (64 scans).

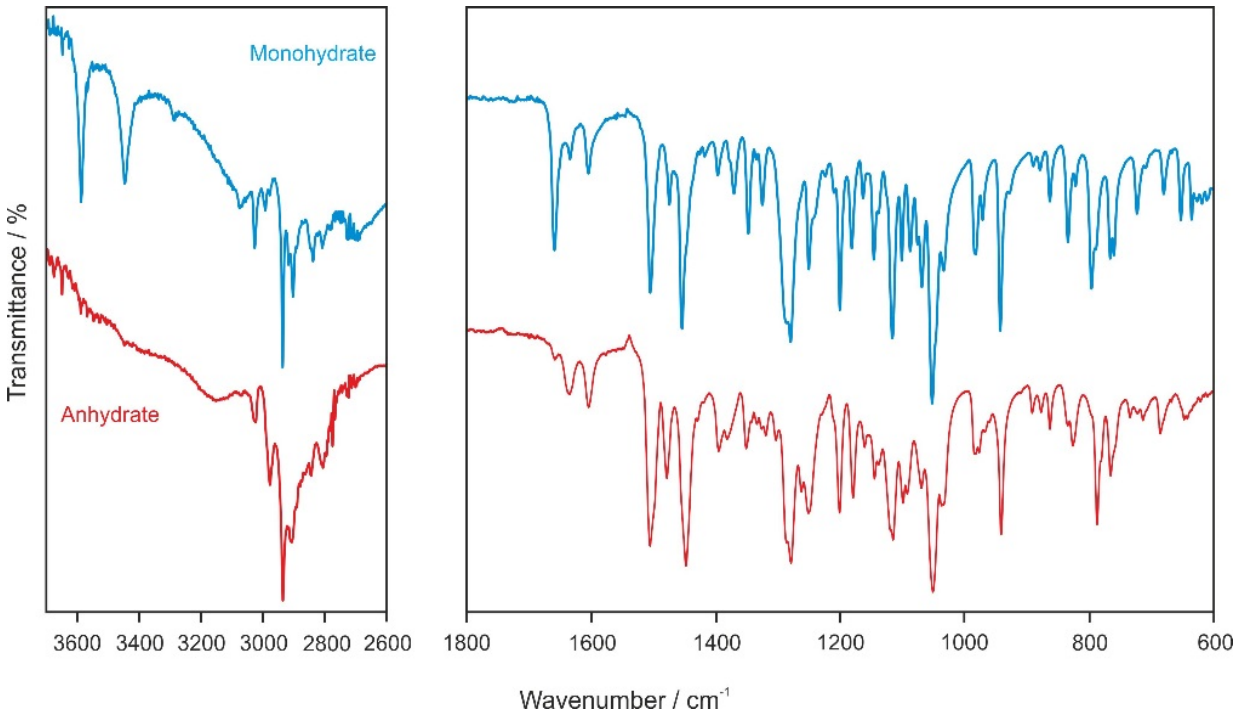

Figure S12. IR spectra of **D**-1H (blue) and **D**-I° (red).

9. Transformation Schemes

9.1.Morphine (M)

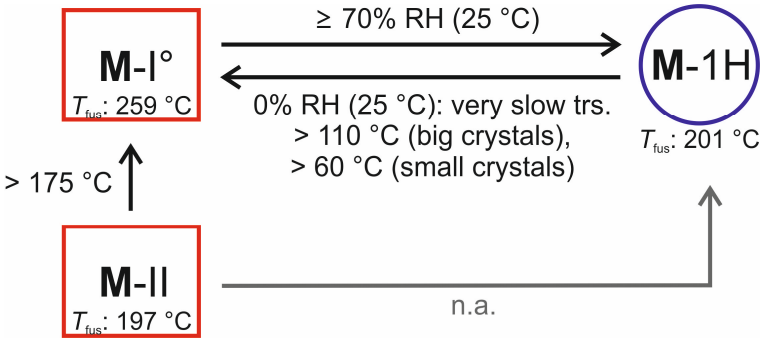

Figure S13. Transformation scheme of morphine solid forms. T_{fus} – melting point, n.a. – not attempted.

9.2. Codeine (C)

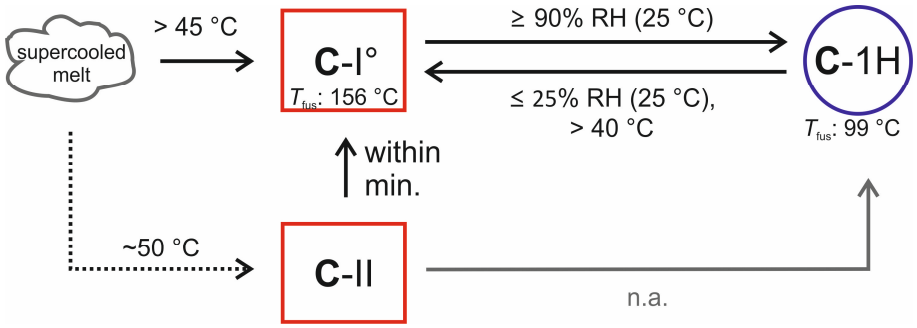

Figure S14. Transformation scheme of codeine solid forms. T_{fus} – melting point, n.a. – not attempted.

9.3. Ethylmorphine (D)

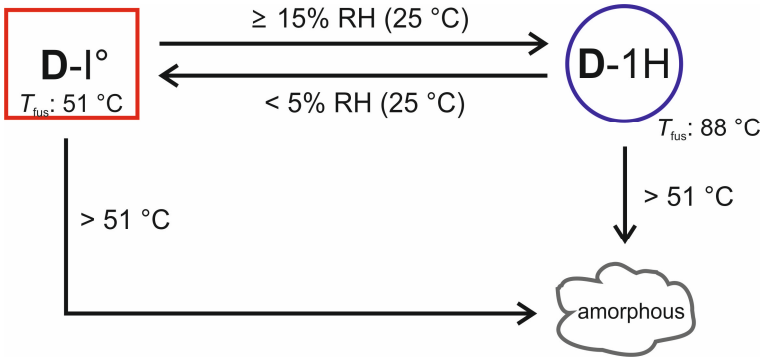

Figure S15. Transformation scheme of ethylmorphine solid forms. T_{fus} – melting point.

9.4. Morphine HCl (M*Cl*)

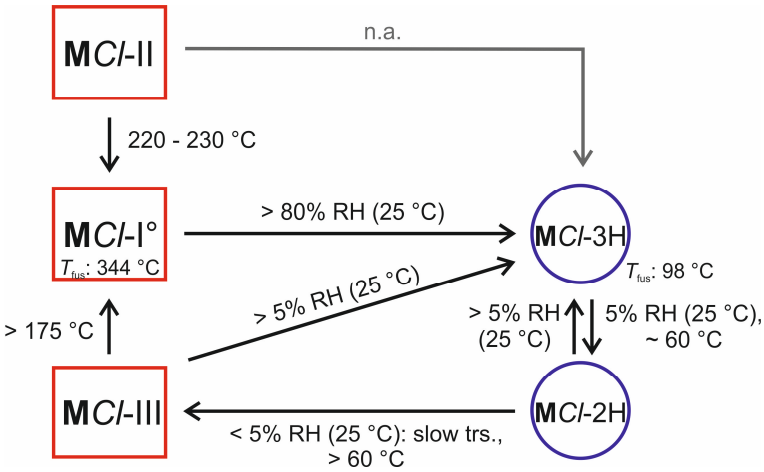

Figure S16. Transformation scheme of morphine HCl solid forms. T_{fus} – melting point, n.a. – not attempted.

9.5. Codeine HCl (C*Cl*)

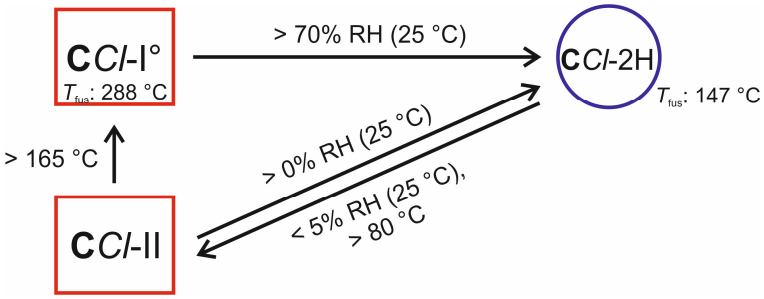

Figure S17. Transformation scheme of codeine HCl solid forms. T_{fus} – melting point.

9.6. Ethylmorphine HCl (D*Cl*)

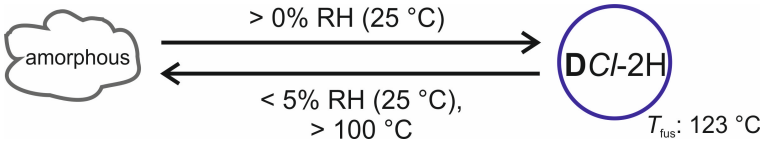

Figure S18. Transformation scheme of ethylmorphine HCl solid forms. T_{fus} – melting point.

B) Computational

10. Conformational Analysis of Morphine (M), Codeine (C) and Ethylmorphine (D)

Conformational energy scans were performed at the SCF/6-31G(d,p) and PBE0/6-31G(d,p) levels of theory using GAUSSIAN09.[8] We considered the main torsion angles depicted in Figure S19 and performed an optimized 1D scan for ϕ_3 (**D**) and 2D scans for the combination of the dihedrals ϕ_1 and ϕ_2 (**M**, **C** and **D**).

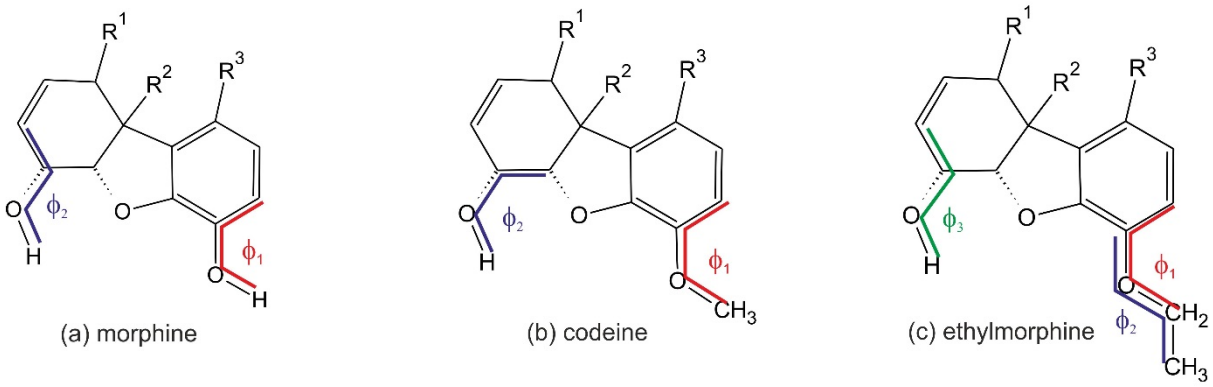

Figure S19. Molecular diagrams of the investigated morphinanes depicting the torsional degrees of freedom.

10.1. Morphine (M)

The 2D scan for the combination of ϕ_1 and ϕ_2 for **M** resulted in three conformational minima (Figure S20). In the global conformational minimum the phenolic OH group adopts a position co-coplanar with the benzene ring with the OH proton pointing towards to the ether oxygen (ϕ_1 = 180 °) and the cyclic OH group forming an intramolecular hydrogen bond with the ether oxygen. The phenolic OH group can rotate significantly for minimal energy cost. A 180° flip of the phenolic OH group results in the second lowest energy conformation (ϕ_1 = 0 °; ca. 9 kJ mol^{-1} less stable than the global conformational energy minimum, calculated at the SCF/6-31 G(d,p) level of theory). The energy barrier between these two conformations was calculated to be less than 14 kJ mol^{-1}. A higher energy barrier was calculated for breaking the intramolecular hydrogen bond, i.e. approx. 20 kJ mol^{-1}. The lowest energy conformation exhibiting no intramolecular O3–H···O1 hydrogen bond (the 3rd minimum) was found to be approx. 17 kJ mol^{-1} less favorable than the global minimum conformation, with the phenolic OH group being

co-planar with the benzene ring and pointing towards to the ether oxygen (as observed in the global conformational energy minimum).

The experimentally observed conformations of the **M***Cl* structures can the related to the global energy minimum region (Figure S20), although differ from the global minimum conformation, due to the presence of the Cl^- ion in the structures. In **M**-I° the morphine molecule adopts a conformation similar to the second lowest energy conformation (intramolecular hydrogen-bonded conformation) and in **M**-1H a high energy conformation, due to the loss of the intramolecular hydrogen bond. The PCM (polarizable continuum model, using a dielectric constant of ε=3) slightly lowers the energy barriers (Figure S20b), but the shape of the potential energy surface landscape is preserved.

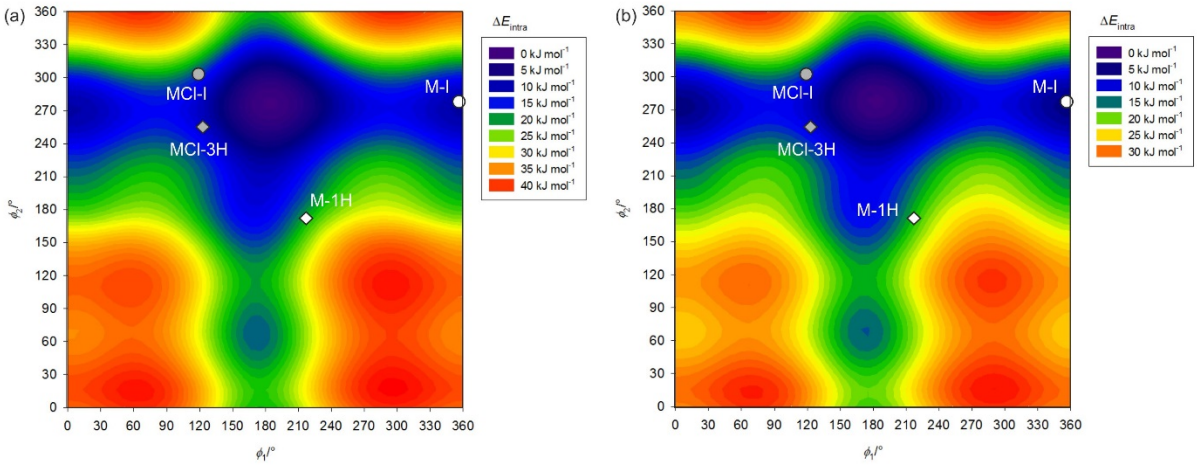

Figure S20. 2D potential energy surface scans for **M** with respect to ϕ_1 and ϕ_2 (Figure S19a) at (a) the SCF level of theory with the 6-31G(d,p) basis set and (b) PCM model (ε=3) using SCF/6-31G(d,p), with the rest of the molecule optimized at each value of ϕ, which was calculated every 20°. Experimental conformations are indicated with diamonds and circles.

10.2. Codeine (C)

The 2D conformational energy scan of ϕ_1 and ϕ_2 for **C** resulted in three low energy conformations, all exhibiting the O3–H···O1 intramolecular hydrogen bond and differing each by 120° rotation of the ϕ_1 torsion Figure S21). The energy barrier for a 360° rotation was calculated to the less than 7 kJ mol^{-1} (SCF/6-31 G(d,p) level of theory). The lowest energy conformation, exhibiting no O3–H···O1 intramolecular hydrogen bond was estimated to be approx. 22 kJ mol^{-1} (SCF/6-31 G(d,p) level of theory) higher in energy than the global

conformational minimum. The PCM (polarizable continuum model, using a dielectric constant of ε=3) slightly narrows the energy barriers (Figure S21b) in contrast to Figure S21a, but the shape of the potential energy surface landscape is preserved.

Three of the experimentally observed conformations (**C**- I°, **C***Cl*-I° and **C***Cl*-2H) can be related to the low energy conformations exhibiting an intramolecular O3–H···O1 hydrogen bond, although the **C***Cl*-I° conformation differs significantly from the closest related low energy conformations (Figure S21). The molecular conformation observed in **C**-1H is a high energy conformation, as O3–H forms an intermolecular hydrogen bond.

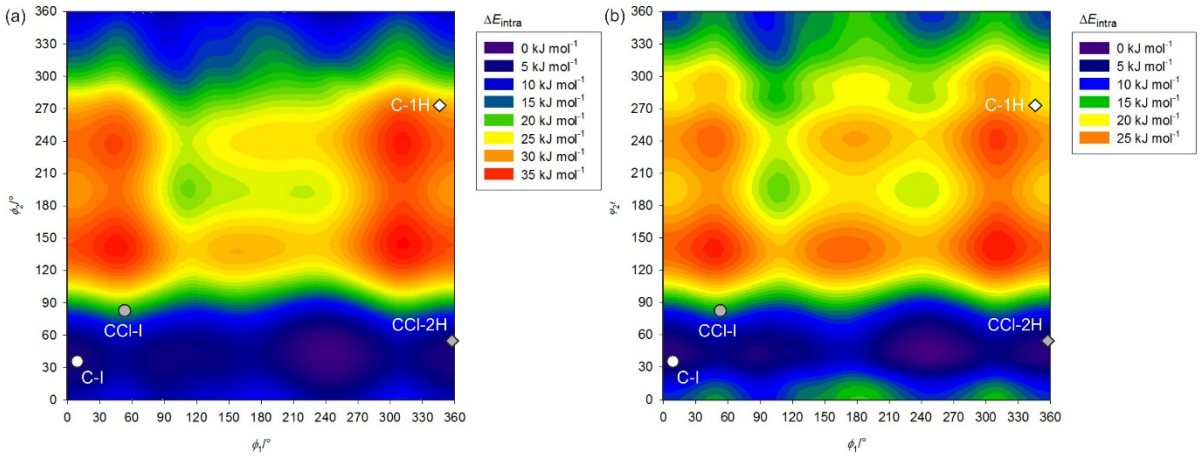

Figure S21. 2D potential energy surface scans for **C** with respect to ϕ_1 and ϕ_2 (Figure 19b) at (a) the SCF level of theory with the 6-31G(d,p) basis set and (b) PCM model (ε=3) using SCF/6-31G(d,p), with the rest of the molecule optimized at each value of ϕ, which was calculated every 20°. Experimental conformations are indicated with diamonds and circles.

10.3. Ethylmorphine (D)

The 1D scan of the C7–C6–O3–H torsion (ϕ_3, Figure 22) exhibits a broad minimum arising from the intramolecular hydrogen bond, i.e the –OH group can move significantly for minimal energy cost. A significant energy barrier is observed for breaking the intramolecular hydrogen bond. This energy barrier can be compensated by the formation of an additional intermolecular hydrogen bond, as in **D**-1H (ϕ_3 = 128°). In **D***Cl*-2H ϕ_3 = 297°.

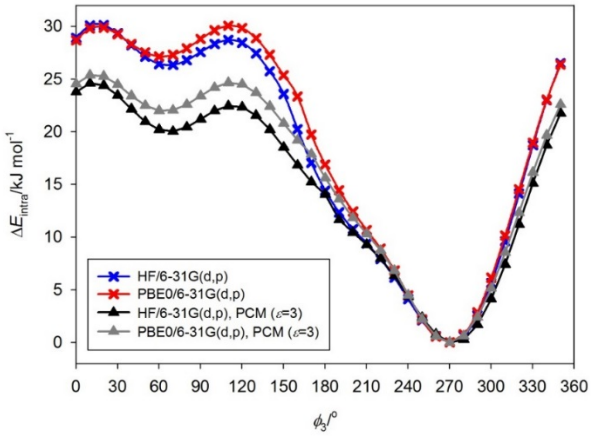

Figure S22. 1D potential energy surface scans for **D** with respect to ϕ_3 (Figure S19c) at the SCF/6-31G (d,p) and PBE0/6-31G(d,p) levels of theory.

The ethoxy-group of the **D** molecule (ϕ_1, Figure S19c) can rotate significantly with minimal energy cost. The energy barrier for a 360° rotation was calculated to be less than 8 kJ mol^{-1} (Figure S23, SCF/6-31 G(d,p) level of theory). The energetically most favourable orientation for ϕ_1 (Figure 19c) = 180° and is observed in all experimental structures. Also ϕ_2 can rotate significantly for minimal energy cost.

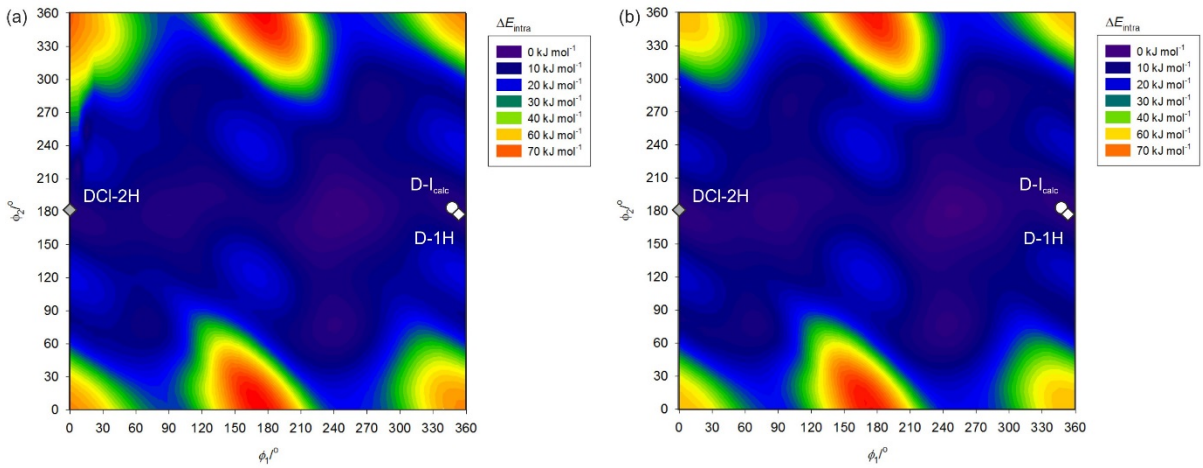

Figure S23. 2D potential energy surface scans for **D** with respect to ϕ_1 and ϕ_2 (Figure S19c) at (a) the SCF level of theory with the 6-31G(d,p) basis set and (b) PCM model (ε=3) using SCF/6-31G(d,p), with the rest of the molecule optimized at each value of ϕ, which was calculated every 20°. Experimental conformations are indicated with diamonds and circles.

11. Periodic Electronic Structure Calculations (DFT-D): Modelling Details

Brillouin zone integrations were performed on a symmetrized Monkhorst–Pack *k*-point grid with the number of *k*-points chosen to provide a maximum spacing of 0.07 $Å^{-1}$. The basis set cut-off (780 eV) and *k*-point spacing were chosen after convergence studies of the total energy of the **M**-I° and **M***Cl*-3H crystal structures. The self-consistent field convergence on total energy was set to $1x10^{-5}$ eV for all minimizations and single-point calculations. Energy minimizations were performed using the Broyden–Fletcher–Goldfarb–Shanno optimization scheme within the space group constraints of the experimentally determined crystal structures. Minimizations were considered complete when energies were converged to better than $2x10^{-5}$ eV per atom, atomic displacements converged to $1x10^{-3}$ Å, maximum forces to $5x10^{-2}$ eV $Å^{-1}$, and, when the unit cell was relaxed, maximum stresses were converged to $1x10^{-1}$ GPa. Energy minimizations with variable unit cells were restarted after the first minimization to reduce the effects of changes in unit cell on the basis set. Isolated molecule minimizations to compute the isolated molecule energy (E_{gas}) were performed by placing a single molecule in a fixed cubic 35x35x35 $Å^3$ unit cell with the same settings as used for the crystal optimization calculations.

12. Representation of the Experimental Structures

The computational model (DFT-TS) was successful in reproducing the experimental structures of the six investigated morphinanes (Table S23).

Table S23. Quality of representation of the experimental structures (all $P2_12_12_1$). Standard settings are used for all structures.

Solid Form, *Temp*	Lattice parameters (cell vectors/Å)			cell density (g cm^{-3})	rmsd$_{15}$[a] (Å)
	a	*b*	*b*		
M-I°, *173 K*	7.699	12.737	13.740	1.407	
M-I°$_{calc}$, *0 K*	7.671	12.612	13.655	1.435	0.06
M-1H, *25 K*	7.431	13.769	14.944	1.318	
M-1H$_{calc}$, *0 K*	7.306Figure	13.659	14.653	1.378	0.12
C-I°, *20 K*	7.335	13.647	14.735	1.348	
C-I°$_{calc}$, *0 K*	7.282	13.528	14.594	1.383	0.08
C-1H, *173 K*	10.399	12.567	12.064	1.337	
C-1H$_{calc}$, *0 K*	10.294	12.050	12.452	1.365	0.06
D-1H, *173 K*	7.082	13.149	18.058	1.309	
D-1H$_{calc}$, *0 K*	6.981	13.144	17.733	1.353	0.09
M*Cl*-I°, *173 K*	7.350	12.852	16.037	1.411	
M*Cl*-I°$_{calc}$, *0 K*	7.274	12.799	16.010	1.434	0.05
M*Cl*-3H, *RT*	6.941	13.019	20.750	1.331	
M*Cl*-3H$_{calc}$, *0 K*	6.721	13.168	20.566	1.372	0.35
C*Cl*-I°, *173 K*	7.144	13.230	16.541	1.427	
C*Cl*-I°$_{calc}$, *0 K*	7.105	13.226	16.412	1.446	0.05
C*Cl*-2H, *123 K*	6.762	12.932	20.308	1.391	
C*Cl*-2H$_{calc}$, *0 K*	6.677	12.895	20.261	1.416	0.08
D*Cl*-2H, *173 K*	6.872	13.392	20.418	1.364	
D*Cl*-2H$_{calc}$, *0 K*	6.775	13.302	20.247	1.405	0.08

[a]Reproduction of the crystal structures was evaluated by the optimal root-mean square overlay of all non-hydrogen atoms in a 15 molecule coordination cluster (rmsd$_{15}$).

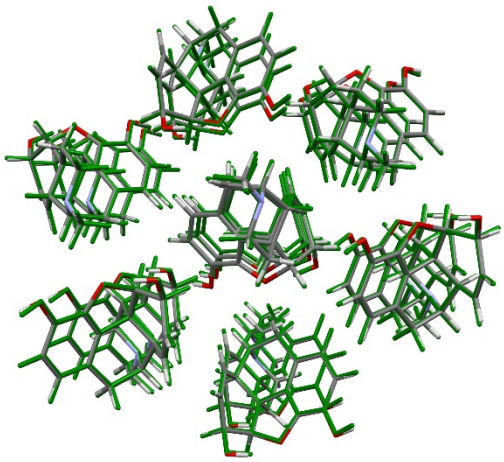

Figure S24. Overlay of the 15 molecule cluster of the observed structure of **M**-I° (colored by element) and calculated DFT-TS structure (green), rmsd$_{15}$=0.06 Å.

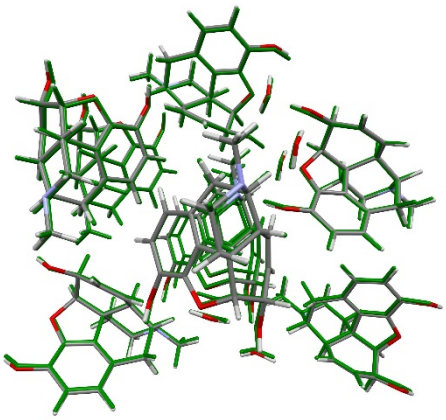

Figure S25. Overlay of the 15 molecule cluster of the observed structure of **M**-1H (colored by element) and calculated DFT-TS structure (green), $rmsd_{15}$=0.12 Å.

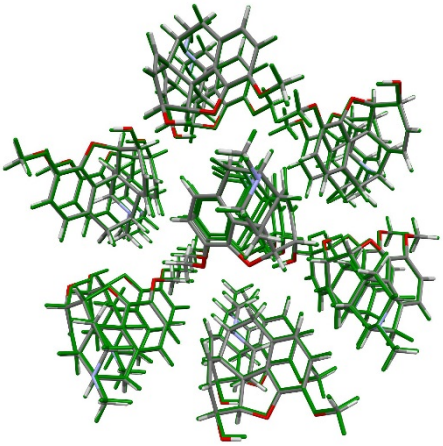

Figure S26. Overlay of the 15 molecule cluster of the observed structure of **C**-I° (colored by element) and calculated DFT-TS structure (green), $rmsd_{15}$=0.08 Å.

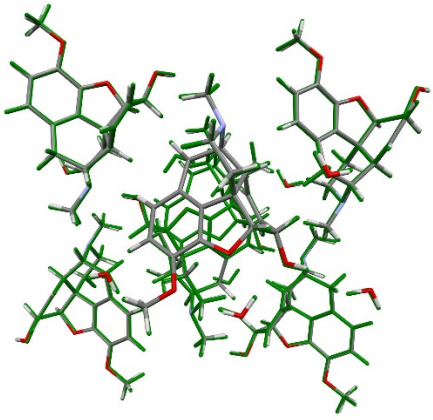

Figure S27. Overlay of the 15 molecule cluster of the observed structure of **C**-1H (colored by element) and calculated DFT-TS structure (green), $rmsd_{15}$=0.06 Å.

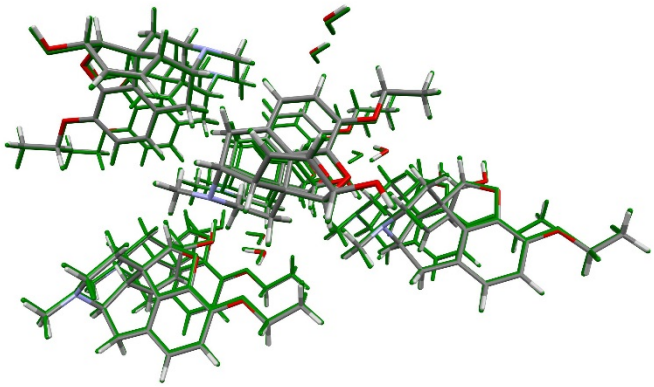

Figure S28. Overlay of the 15 molecule cluster of the observed structure of **D**-1H (colored by element) and calculated DFT-TS structure (green), $rmsd_{15}$=0.09 Å.

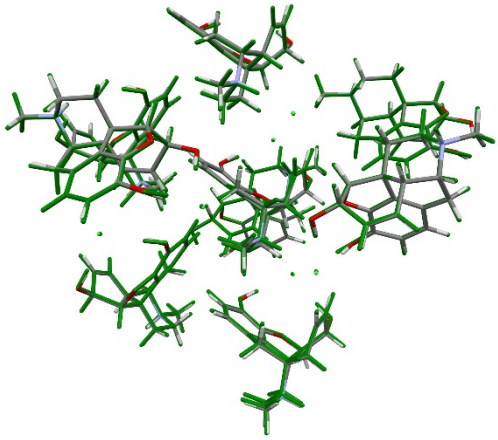

Figure S29. Overlay of the 15 molecule cluster of the observed structure of **M***Cl*-I° (colored by element) and calculated DFT-TS structure (green), $rmsd_{15}$=0.05 Å.

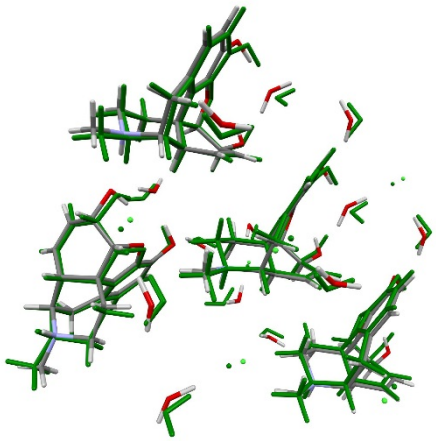

Figure S30. Overlay of the 30 molecule cluster of the observed structure of **M***Cl*-3H (colored by element) and calculated DFT-TS structure (green), $rmsd_{30}$=0.34 Å. For differences see Figure 12.

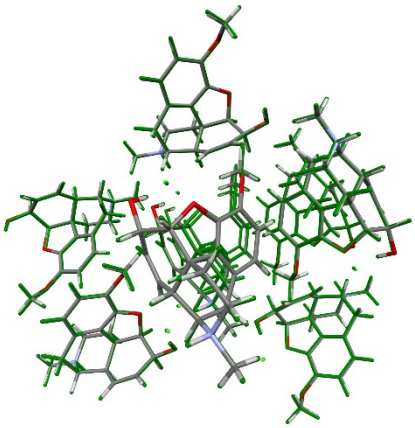

Figure S31. Overlay of the 15 molecule cluster of the observed structure of **C***Cl*-I° (colored by element) and calculated DFT-TS structure (green), $rmsd_{15}$=0.05 Å.

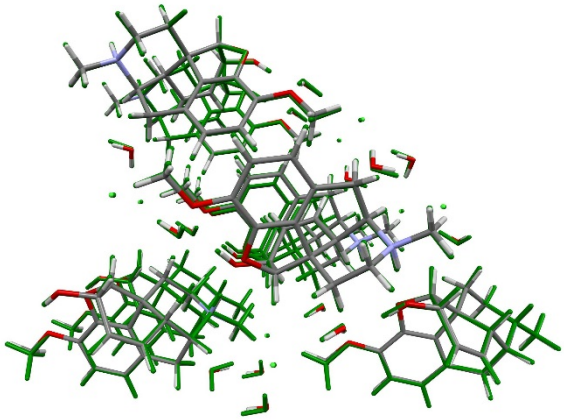

Figure S32. Overlay of the 30 molecule cluster of the observed structure of **C***Cl*-2H (colored by element) and calculated DFT-TS structure (green), $rmsd_{30}$=0.08 Å.

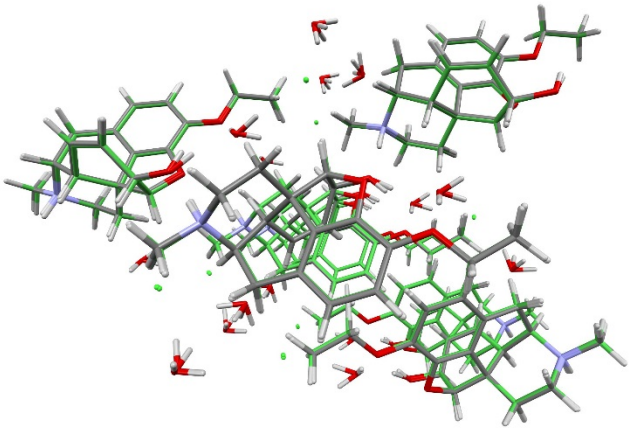

Figure S33. Overlay of the 30 molecule cluster of the observed structure of **D***Cl*-2H (colored by element) and calculated DFT-TS structure (green), $rmsd_{30}$=0.08 Å.

13. Computational Dehydration

The lattice energy (E_{latt}) was calculated from the total periodic *ab initio* energy per molecule minus E_{gas} (opt). Computationally we can generate hypothetical lower-stoichiometric hydrate and framework (FW) structures by removing water molecule(s). By comparing E_{latt} of the hydrate and the FW_{fix} structure (single point calculation, cell and atomic positions fixed) the contribution of the water molecule to the hydrate lattice energy can be estimated. Comparing E_{latt} of the hydrate to E_{latt} of the optimized FW structure (FW_{opt}) and ice, and comparing E_{latt} of the experimental anhydrate to FW_{opt} can give insights into the likelihood of the existence of an isomorphic desolvate and thus the dehydration mechanism. Details of the computational dehydration calculations are given in Table S24 for the free bases and Table S25 for the HCl salts.

Table S24. Computational Dehydration of **M**-1H, **C**-1H and **D**-1H.

Solid Form[a]	a	b	c	density	E_{latt}	$\Delta_{dehy}U_{X\text{-}Y}$[c]	$\Delta_{trs}U_{X\text{-}Y}$[d]	X, Y
	/Å			/g cm^{-3}	/kJ mol^{-1}			
Morphine (**M**)								
M-1H, *25 K*	7.431	13.769	14.944	1.318	–	–	–	–
M-$1H_{calc}$	7.306	13.659	14.653	1.378	−281.01	–	–	–
M-FW_{fix}	7.306	13.659	14.653	1.296	−158.33	+122.69	+63.69	X=1H, Y=FW_{fix}
M-FW_{opt}(inter)	7.129	14.067	14.329	1.319	−170.92	+110.09	+51.09	X=1H, Y=FW_{opt}
M-FW_{opt}(intra)	7.246	13.712	14.596	1.307	−180.59	+100.42	+41.42	X=1H, Y=FW_{opt}
M-I°, *173 K*	7.699	12.737	13.740	1.407	–	–	–	–
M-$I°_{calc}$	7.671	12.612	13.655	1.435	−201.18	+79.83	+20.83	X=1H, Y=I°
Codeine (**C**)								
C-1H, *173 K*	10.399	12.567	12.064	1.337	–	–	–	–
C-$1H_{calc}$	10.294	12.050	12.452	1.365	−246.65	–	–	–
C-FW_{fix}	10.294	12.050	12.452	1.287	−158.67	+87.98	+28.98	X=1H, Y=FW_{fix}
C-FW_{opt}(inter)	10.288	11.837	12.685	1.287	−161.65	+85.00	+26.00	X=1H, Y=FW_{opt}
C-FW_{opt}(intra)	10.577	11.013	13.019	1.311	−158.94	+87.71	+28.71	X=1H, Y=FW_{opt}
C-I°, *20 K*	7.335	13.647	14.735	1.348	–	–	–	–
C-$I°_{calc}$	7.282	13.528	14.594	1.383	−182.09	+64.57	+5.57	X=1H, Y= I°
Ethylmorphine (**D**)								
D-1H, *173 K*	7.082	13.149	18.058	1.309	–	–	–	–
D-$1H_{calc}$	6.981	13.144	17.733	1.353	−266.27	–	–	–
D-FW_{fix}	6.981	13.144	17.733	1.279	−177.26	+89.01	+30.01	X=1H, Y=FW_{fix}
D-FW_{opt}(inter)	7.344	13.183	15.868	1.355	−194.98	+71.30	+12.30	X=1H, Y=FW_{opt}
D-FW_{opt}(intra)	7.097	13.258	17.477	1.266	−154.08	+112.19	+53.19	X=1H, Y=FW_{opt}
D-I°, *298 K*[b]	7.417	13.271	16.273	1.300	–	–	–	–
D-$I°_{calc}$	7.344	13.183	15.868	1.355	−194.98	+71.30	+12.30	X=1H, Y=I°

[a]FW – all framework structures are calculated structures, fix – fixed cell, opt – full structure optimization, inter – C-C-O3-H forming an intermolecular hydrogen bond, intra – C-C-O3-H forming an intramolecular hydrogen bond. [b]Cell parameters derived from indexing the PXRD pattern. [c]$\Delta_{dehy}U_{X-Y} = -E_{latt(X)} - (-E_{latt(Y)})$. [d]$\Delta_{trs}U_{X-Y} = \Delta_{dehy}U_{X-Y} - n(-E_{latt(ice)})$, with *n* corresponding to the difference of water molecules per mol of **M**/**C**/**D**.

Table S25. Computational Dehydration of **M***Cl*, **C***Cl* and **D***Cl* Hydrates.

Solid Form[a]	a	b	c	density	E_{latt}	$\Delta_{dehy}U_{X\text{-}Y}$[d]	$\Delta_{trs}U_{X\text{-}Y}$[e]	X, Y
		/Å		/g cm^{-3}		/kJ mol^{-1}		
Morphine HCl (**M***Cl*)								
M*Cl*-3H, *RT*	6.941	13.019	20.750	1.331	–	–	–	–
M*Cl*-3H$_{calc}$	6.721	13.168	20.566	1.372	−959.34	–	–	–
M*Cl*-2H, *RT*[b]	6.937	12.452	19.819	1.388	–	–	–	–
M*Cl*-2H-A$_{fix}$	6.721	13.168	20.566	1.306	−865.11	+94.23	+35.23	X=3H, Y=2H-Afix
M*Cl*-2H-A$_{opt}$	6.714	12.746	19.915	1.371	−900.83	+58.51	−0.49	X=3H, Y=2H-Aopt
M*Cl*-2H-B$_{fix}$	6.721	13.168	20.566	1.306	−871.59	+87.75	+28.75	X=3H, Y=2H-Bfix
M*Cl*-2H-B$_{opt}$	6.706	12.753	20.277	1.395	−884.44	+74.90	+15.90	X=3H, Y=2H-Bopt
M*Cl*-2H-C$_{fix}$	6.721	13.168	20.566	1.306	−832.06	+127.28	+68.28	X=3H, Y=2H-Cfix
M*Cl*-2H-C$_{opt}$[c]	6.762	12.901	19.536	1.395	−913.56	+45.78	−13.22	X=3H, Y=2H-Copt
M*Cl*-1H-B$_{fix}$	6.714	12.746	19.915	1.324	−821.46	+79.37	+20.37	X=2H-Bopt, Y=1H-Bfix
M*Cl*-1H-B$_{opt}$	6.753	12.493	19.554	1.368	−826.54	+74.29	+15.29	X=2H-Bopt, Y=1H-Bopt
M*Cl*-1H-C$_{fix}$	6.714	12.746	19.915	1.324	−785.14	+115.69	+56.69	X=2H-Bopt, Y=1H-Cfix
M*Cl*-1H-C$_{opt}$[c]	6.946	12.531	18.274	1.419	−834.06	+66.77	+7.94	X=2H-Bopt, Y=1H-Copt
M*Cl*-FW$_{fix}$	6.721	13.168	20.566	1.174	−665.94	+160.60	+101.60	X=1H-Copt, Y=FWfix
M*Cl*-FW$_{opt}$	6.801	12.106	19.148	1.356	−772.50	+54.03	−4.97	X=1H-Copt, Y=FWopt
M*Cl*-I°, *173 K*	7.350	12.852	16.037	1.411	–	–	–	–
M*Cl*-I°$_{calc}$	7.274	12.799	16.010	1.434	−805.45	+153.89	−23.11	X=3H, Y= I°
Codeine HCl (**C***Cl*)								
C*Cl*-2H,*123 K*	6.762	12.932	20.308	1.391	–	–	–	–
C*Cl*-2H$_{calc}$	6.677	12.895	20.261	1.416	−937.74	–	–	–
C*Cl*-1H-B$_{fix}$	6.677	12.895	20.261	1.347	−849.93	+87.82	+28.82	X=2H, Y=1H-Bfix
C*Cl*-1H-B$_{opt}$	6.686	12.730	20.102	1.374	−854.31	+83.44	+24.44	X=2H, Y=1H-Bopt
C*Cl*-1H-C$_{fix}$	6.677	12.895	20.261	1.347	−819.89	+117.85	+58.85	X=2H, Y=1H-Cfix
C*Cl*-1H-C$_{opt}$	6.740	12.973	19.724	1.363	−834.46	+103.29	+44.29	X=2H, Y=1H-Copt
C*Cl*-FW$_{fix}$	6.677	12.895	20.261	1.279	−721.80	+128.13	+69.13	X=1H-Copt, Y=FWfix
C*Cl*-FW$_{opt}$	6.724	12.742	19.432	1.340	−744.54	+109.77	+50.77	X=1H-Copt, Y=FWopt
C*Cl*-I°, *173 K*	7.144	13.230	16.541	1.427	–	–	–	–
C*Cl*-I°$_{calc}$	7.105	13.226	16.412	1.446	−798.18	+139.57	+21.57	X=2H, Y=I°
Ethylmorphine HCl (**D***Cl*)								
D*Cl*-2H,*173 K*	6.872	13.392	20.418	1.364	–	–	–	–
D*Cl*-2H$_{calc}$	6.775	13.302	20.247	1.405	−943.41	–	–	–
D*Cl*-1H-B$_{fix}$	6.775	13.302	20.247	1.339	−857.25	+86.16	+27.16	X=2H, Y=1H-Bfix
D*Cl*-1H-B$_{opt}$	6.741	13.097	20.294	1.364	−865.69	+77.72	+18.72	X=2H, Y=1H-Bopt
D*Cl*-1H-C$_{fix}$	6.775	13.302	20.247	1.339	−829.01	+114.40	+55.40	X=2H, Y=1H-Cfix
D*Cl*-1H-C$_{opt}$	6.837	13.530	19.560	1.350	−846.01	+97.40	+38.40	X=2H, Y=1H-Copt
D*Cl*-FW$_{fix}$	6.775	13.302	20.247	1.273	−735.40	+121.85	+62.85	X=1H-Copt, Y=FWfix
D*Cl*-FW$_{opt}$	6.749	13.285	19.848	1.305	−755.72	+109.96	+50.96	X=1H-Copt, Y=FWopt
D*Cl*-I$_{calc}$	7.241	13.950	17.571	1.309	−746.46	+196.95	+78.95	X=2H, Y=I°

[a]RT – room temperature, **M***Cl*-2H-A$_{opt}$ corresponds to **M***Cl*-2H$_{calc}$, fix – fixed cell, opt – full structure optimization. [b]Cell parameters derived from indexing the PXRD pattern. [c]Change in structure upon optimization: Cl^- ion takes place of water molecule (no isostructural structure). [d]$\Delta_{dehy}U_{X-Y} = -E_{latt(X)} - (-E_{latt(Y)})$. [e]$\Delta_{trs}U_{X-Y} = \Delta_{dehy}U_{X-Y} - n(-E_{latt(ice)})$, with *n* corresponding to the difference of water molecules per mol of **M***Cl*/**C***Cl*/**D***Cl*.

14. Void space analysis

The computationally generated anhydrate (I°), hydrate (3H, 2H, 1H) and framework structures (FW_{fix}, FW_{opt}) were subjected to void space calculations using a 1 Å probe radius and an approximate grid spacing of 0.1 Å using Mercury (Table S26 and S27).

Table S26. Void space calculations of **M**, **C** and **D** structures with water molecules removed.

Compound	I°	1H	FW_{fix}[a]	FW_{opt}
	Void Space / %/Å^3			
M	0/0	3.6/53.11	6.4/93.59 (2.8/40.48)	5.9/85.29
C	0/0	0/0	7.0/107.03	7.0/107.53
D	–	1.7/28.0	7.0/113.74 (5.3/85.74)	0/0

[a]Values in parenthesis are calculated as void space of FW minus void space of 1H.

Table S27. Void space calculations for **M***Cl*, **C***Cl* and **D***Cl* structures with water molecules partially and completely removed.

Cpd	I°	3H	2H	1H	FW_{fix}	FW_{opt}
	Void Space / %/Å^3					
M*Cl*	0/0	1.4/24.95	A: 1.0/23.41 B: 2.4/41.92 C: 0.4/7.07	B: 5.3/88.18 C: 2.3/36.03	16.3/297.13	9.7/152.97
C*Cl*	0/0	–	0/0	B: 2.8/48.50 C: 5.7/96.86	8.0/39.91	6.1/101.92
D*Cl*	1.7/30.58	–	0/0	B: 5.1/91.75 C: 5.5/98.81	9.6/175.88	9.2/164.42

15. Computationally Generated D-I° Structure

The .res file for the computationally generated **D**-I° is given:

```
TITL Dionine_AH_DFT
CELL  1.54180   7.3439   13.1829   15.8681   90.000   90.000   90.000
ZERR      4   0.0000   0.0000   0.0000    0.000    0.000    0.000
LATT  -1
SYMM     0.50000 - X ,          - Y ,    0.50000 + Z
SYMM     0.50000 + X ,    0.50000 - Y ,          - Z
SYMM           - X ,    0.50000 + Y ,    0.50000 - Z
SFAC  C  H  N  O
C1    1  0.12324  0.50758  0.50005  11.00000   0.0500
C2    1  0.11508  0.61271  0.48964  11.00000   0.0500
C3    1  0.19620  0.66122  0.42031  11.00000   0.0500
C4    1  0.27931  0.59834  0.36082  11.00000   0.0500
C5    1  0.48009  0.53750  0.26464  11.00000   0.0500
C6    1  0.67729  0.53949  0.30284  11.00000   0.0500
C7    1  0.71133  0.46260  0.37042  11.00000   0.0500
C8    1  0.61921  0.37600  0.37916  11.00000   0.0500
C9    1  0.31581  0.28300  0.36720  11.00000   0.0500
C10   1  0.23540  0.33329  0.44722  11.00000   0.0500
C11   1  0.20400  0.44552  0.43913  11.00000   0.0500
C12   1  0.22364  0.41459  0.22644  11.00000   0.0500
C13   1  0.08720  0.33941  0.26190  11.00000   0.0500
C14   1  0.46168  0.34989  0.32364  11.00000   0.0500
C15   1  0.27290  0.49420  0.36889  11.00000   0.0500
C16   1  0.36364  0.44634  0.29367  11.00000   0.0500
C17   1  0.04331  0.18115  0.33452  11.00000   0.0500
C18   1  0.09300  0.82583  0.46239  11.00000   0.0500
C19   1  0.11780  0.93460  0.43560  11.00000   0.0500
H1    2  0.74263  0.68305  0.28347 11.00000 -1.50000
H2    2  0.06675  0.47410  0.55728 11.00000 -1.20000
H3    2  0.15085  0.48139  0.20250 11.00000 -1.20000
H4    2  0.29690  0.38071  0.17287 11.00000 -1.20000
H5    2  0.82788  0.47995  0.41050 11.00000 -1.20000
H6    2  0.51109  0.30635  0.26867 11.00000 -1.20000
H7    2  0.48835  0.54358  0.19572 11.00000 -1.20000
H8    2  0.38177  0.21168  0.38696 11.00000 -1.20000
H9    2 -0.00553  0.37800  0.30633 11.00000 -1.20000
H10   2  0.00099  0.30780  0.21185 11.00000 -1.20000
H11   2  0.76755  0.51779  0.24954 11.00000 -1.20000
H12   2  0.25379  0.96252  0.45170 11.00000 -1.50000
H13   2  0.09820  0.94268  0.36749 11.00000 -1.50000
H14   2  0.01735  0.98210  0.46809 11.00000 -1.50000
H15   2  0.66039  0.32171  0.42749 11.00000 -1.20000
H16   2 -0.05939  0.21618  0.37627 11.00000 -1.50000
H17   2  0.11115  0.11992  0.36909 11.00000 -1.50000
H18   2 -0.03050  0.14878  0.28073 11.00000 -1.50000
H19   2  0.13237  0.81632  0.52889 11.00000 -1.20000
H20   2 -0.04927  0.80139  0.45465 11.00000 -1.20000
H21   2  0.10948  0.29379  0.46550 11.00000 -1.20000
H22   2  0.33080  0.32003  0.49972 11.00000 -1.20000
H23   2  0.04754  0.65827  0.53759 11.00000 -1.20000
N1    3  0.17868  0.25313  0.30321  11.00000   0.0500
O1    4  0.37701  0.62782  0.29111  11.00000   0.0500
O2    4  0.20581  0.76348  0.40841  11.00000   0.0500
O3    4  0.72862  0.63612  0.33350  11.00000   0.0500
END
```

16. Computationally Generated M*Cl*-2H

The .res file for the computationally generated **M***Cl*-2H is given:

```
TITL MCl_DH
CELL  1.54180    6.7143   12.7463   19.9152    90.000    90.000    90.000
ZERR       4    0.0000    0.0000    0.0000     0.000     0.000     0.000
LATT  -1
SYMM     0.50000 - X ,           - Y ,    0.50000 + Z
SYMM     0.50000 + X ,    0.50000 - Y ,           - Z
SYMM           - X ,    0.50000 + Y ,    0.50000 - Z
SFAC  C  H Cl  N  O
C1    1  0.99269  0.33819  0.47379  11.00000   0.0500
C2    1  1.00181  0.23001  0.46333  11.00000   0.0500
C3    1  0.91824  0.18295  0.40627  11.00000   0.0500
C4    1  0.84274  0.25120  0.35802  11.00000   0.0500
C5    1  0.65029  0.31633  0.27267  11.00000   0.0500
C6    1  0.42469  0.30703  0.28573  11.00000   0.0500
C7    1  0.36404  0.34923  0.35296  11.00000   0.0500
C8    1  0.44170  0.43795  0.37734  11.00000   0.0500
C9    1  0.72839  0.56934  0.38141  11.00000   0.0500
C10   1  0.84532  0.51772  0.43914  11.00000   0.0500
C11   1  0.90201  0.40496  0.42684  11.00000   0.0500
C12   1  0.90061  0.46671  0.26307  11.00000   0.0500
C13   1  1.00834  0.55531  0.29872  11.00000   0.0500
C14   1  0.60237  0.49320  0.33861  11.00000   0.0500
C15   1  0.84250  0.35834  0.36754  11.00000   0.0500
C16   1  0.74698  0.41139  0.30835  11.00000   0.0500
C17   1  0.96663  0.71956  0.36300  11.00000   0.0500
H1    2  0.77908  0.05826  0.37989 11.00000 -1.50000
H2    2  0.42617  0.15140  0.30358 11.00000 -1.50000
H3    2  0.76906  0.65797  0.29445 11.00000 -1.20000
H4    2  1.05923  0.37028  0.51919 11.00000 -1.20000
H5    2  0.74783  0.52155  0.48358 11.00000 -1.20000
H6    2  0.97571  0.56537  0.45270 11.00000 -1.20000
H7    2  0.53294  0.54007  0.29815 11.00000 -1.20000
H8    2  1.01369  0.41025  0.24619 11.00000 -1.20000
H9    2  0.82629  0.49605  0.21758 11.00000 -1.20000
H10   2  1.09503  0.60290  0.26341 11.00000 -1.20000
H11   2  1.10951  0.52580  0.33762 11.00000 -1.20000
H12   2  1.04410  0.76110  0.32274 11.00000 -1.50000
H13   2  0.85444  0.77072  0.38575 11.00000 -1.50000
H14   2  1.07574  0.69338  0.40020 11.00000 -1.50000
H15   2  1.06694  0.17947  0.50149 11.00000 -1.20000
H16   2  0.67467  0.31551  0.21819 11.00000 -1.20000
H17   2  0.35373  0.35410  0.24569 11.00000 -1.20000
H18   2  0.24832  0.30691  0.37995 11.00000 -1.20000
H19   2  0.39030  0.47160  0.42470 11.00000 -1.20000
H20   2  0.63155  0.63075  0.40201 11.00000 -1.20000
Cl1   3  0.51571  0.32629  0.09927  11.00000   0.0500
N1    4  0.86350  0.62763  0.33256  11.00000   0.0500
O1    5  0.75094  0.22238  0.29904  11.00000   0.0500
O2    5  0.91075  0.07609  0.39969  11.00000   0.0500
O3    5  0.35465  0.20250  0.27436  11.00000   0.0500
H21   2  0.57857  0.58305  0.09859 11.00000 -1.50000
H22   2  0.51609  0.47420  0.12787 11.00000 -1.50000
O4    5  0.50257  0.55261  0.13579  11.00000   0.0500
H23   2  0.78550  0.14374 -0.01971 11.00000 -1.50000
H24   2  0.64889  0.19886  0.03433 11.00000 -1.50000
O5    5  0.69867  0.12977  0.01942  11.00000   0.0500
END
```

Reference List

1. Gelbrich, T.; Hursthouse, M. B. *CrystEngComm* **2005,** *7*, 324-336.

2. Gelbrich, T.; Threlfall, T. L.; Hursthouse, M. B. *CrystEngComm* **2012,** *14*, 5454-5464.

3. Gelbrich, T.; Braun, D. E.; Griesser, U. J. *Acta Crystallogr. , Sect. E: Struct. Rep. Online* **2012,** *E68*, o3358-o3359.

4. Gelbrich, T.; Braun, D. E.; Griesser, U. J. *Acta Crystallogr. , Sect. E: Struct. Rep. Online* **2013,** *69*, o2.

5. Scheins, S.; Messerschmidt, M.; Luger, P. *Acta Crystallogr. B* **2005,** *61*, 443-448.

6. Scheins, S.; Messerschmidt, M.; Morgenroth, W.; Paulmann, C.; Luger, P. *J. Phys. Chem. A* **2007,** *111*, 5499-5508.

7. Gylbert, L. *Acta Crystallogr., Sect. B* **1973,** *29*, 1630-1635.

8. *Gaussian 09,* Frisch, M. J.; Trucks, G. W.; Schlegel, H. B.; Scuseria, G. E.; Robb, J. M. A.; Cheeseman, R.; Scalmani, G.; Barone, V.; Mennucci, B.; Petersson, G. A.; Nakatsuji, H.; Caricato, M.; Li, X.; Hratchian, H. P.; Izmaylov, A. F.; Bloino, J.; Zheng, G.; Sonnenberg, J. L.; Hada, M.; Ehara, M.; Toyota, K.; Fukuda, R.; Hasegawa, J.; Ishida, M.; Nakajima, T.; Honda, Y.; Kitao, O.; Nakai, H.; Vreven, T.; Montgomery, J. A.; Peralta, J. E.; Ogliaro, F.; Bearpark, M.; Heyd, J. J.; Brothers, E.; Kudin, K. N.; Staroverov, V. N.; Kobayashi, R.; Normand, J.; Raghavachari, K.; Rendell, A.; Burant, J. C.; Iyengar, S. S.; Tomasi, J.; Cossi, M.; Rega, N.; Millam, J. M.; Klene, M.; Knox, J. E.; Cross, J. B.; Bakken, V.; Adamo, C.; Jaramillo, J.; Gomperts, R.; Stratmann, R. E.; Yazyev, O.; Austin, A. J.; Cammi, R.; Pomelli, C.; Ochterski, J. W.; Martin, R. L.; Morokuma, K.; Zakrzewski, V. G.; Voth, G. A.; Salvador, P.; Dannenberg, J. J.; Dapprich, S.; Daniels, A. D.; Farkas; Foresman, J. B.; Ortiz, J. V.; Cioslowski, J.; Fox, D. J. Gaussian Inc.: Wallingford CT, **2009**